Latest Ordovician-earliest Silurian acritarchs and chitinozoans from subsurface samples in Jebel Asba, Kufra Basin, SE Libya

Bindra Thusu, Sayed Rasul, Florentin Paris, Guido Meinhold, James P. Howard, Youssef Abutarruma, Andrew G. Whitham

Latest Ordovician–earliest Silurian acritarchs and chitinozoans from subsurface samples in Jebel Asba, Kufra Basin, SE Libya

Bindra Thusu[1], Syed Rasul[1], Florentin Paris[2], Guido Meinhold[3,4,*], James P. Howard[3], Yousef Abutarruma[5], Andrew G. Whitham[3]

[1] Maghreb Petroleum Research Group, Department of Earth Sciences, University College London, Gower Street, London WC1E 6BT, United Kingdom

[2] Rue des Jonquilles, 35235 Thorigné-Fouillard, France; Géosciences Rennes, CNRS UMR 6118, Université de Rennes 1, Rennes cedex, France

[3] CASP, University of Cambridge, West Building, 181A Huntingdon Road, Cambridge CB3 0DH, United Kingdom

[4] Geowissenschaftliches Zentrum der Universität Göttingen, Abteilung Sedimentologie/Umweltgeologie, Goldschmidtstraβe 3, 37077 Göttingen, Germany

[5] Mellitah Oil & Gas B.V., Dat Al Imad Complex Tower 5 Floor 13, P.O. Box 91651, Tripoli, Libya

* Corresponding author: Tel.: +49 551 393455; fax: +49 551 397996.

E-mail address: guido.meinhold@geo.uni-goettingen.de (G. Meinhold)

Abstract

Latest Ordovician–earliest Silurian Tanezzuft Formation shales recovered from core material of the shallow borehole JA-2 drilled in Jebel Asba at the eastern margin of the Kufra Basin, southeastern Libya, yielded well-diversified palynomorph assemblages with transparent and brownish to yellowish vesicles and organic matter (visual kerogen Type 1 and 2) from depth interval 46.20 to 67.82 m. In addition, miospores including cryptospores, and *Tasmanites* sp. ("*Tasmanites* with nodules"), scolecodonts, and a stratigraphically significant palaeo-marker, the enigmatic, tubular organic structure *Tortotubus protuberans*, were also recorded frequently in most samples. Kerogen colour based on miospores (TAI <3) and chitinozoan reflectance indicate an immature facies for oil generation. The two uppermost samples (from 33.33 m and 46.20 m depths) and the lowermost ones (from 67.92 to 73.21 m depth) contain rare palynomorphs and other organic remains and have been partially affected by oxidation.

Furthermore, palynological and palynofacies analysis was carried out on cuttings from an old well (UN-REMSA well), ca. 530 m towards the NNE from well JA-2. The composition of the organic residue is similar in both wells. However, the UN-REMSA well yields fairly numerous chitinozoans, scolecodonts and biofilms but lacks the "thread-like structures" and "*Tasmanites* with nodules" observed in well JA-2.

All the investigated samples in well JA-2 are dominated by a single chitinozoan species, *Euconochitina moussegoudaensis* Paris (in Le Hérissé et al., 2013). Based on correlation with chitinozoan-bearing strata around the Ordovician−Silurian boundary, the analysed samples from well JA-2 and from the UN-REMSA well are regarded as post-glacial, but still of either latest Hirnantian age, or at least no younger than earliest Rhuddanian. A well-diversified acritarch,

miospore and cryptospore assemblage recorded in well JA-2 supports a marginal marine (nearshore) depositional environment. This assemblage is no older than earliest Rhuddanian yet the latest Hirnantian age of the assemblage cannot be completely ruled out as our current knowledge on the post-glacial, latest Hirnantian acritarch and miospore assemblages is poorly documented in North Africa.

Keywords: biostratigraphy; acritarchs; chitinozoans; Hirnantian; Silurian, Gondwana; Libya

Research highlights

► We describe palynomorphs from subsurface shales of SE Libya.

► The shales are of latest Hirnantian–earliest Rhuddanian age.

► The shales are immature for oil generation.

► Dominant chitinozoan species *Euconochitina moussegoudaensis* Paris.

► Discussion of the Ordovician–Silurian boundary.

1. Introduction

The precise location of the source rock horizons close to the Ordovician−Silurian boundary is an important question for hydrocarbon exploration in northern Gondwana regions. In areas of anoxic geological setting, typical "hot shale" horizons are easily identified by their peculiar lithology (e.g., black shales), a sharp positive excursion of the gamma-ray curve in the well logs and high total organic carbon (TOC) content (e.g., Lüning et al., 2000, 2005, 2006). These characteristics can also be determined by the visual nature and the abundance of the organic

matter including palynomorphs, animal remains and associated amorphous organic matter (AOM).

The main goal of the present study is to record for the first time moderately rich to rich assemblages of acritarchs, chitinozoans, miospores and cryptospores recovered from well JA-2 in Jebel Asba, Kufra Basin, drilled by CASP (formerly known as Cambridge Arctic Shelf Programme) in April–May 2009 (Fig. 1).

2. Material and methods

2.1. Sampling

Core samples from well JA-2 (geographic coordinates: 22°35'49.31"N, 24°7'57.10"E) drilled in the Jebel Asba at the eastern margin of the Kufra Basin (Figs 1 and 2) and cuttings (single sample SJS0001) from a pile of drill cuttings surrounding the borehole collar of an abandoned well (geographic coordinates: 22°36'4.52"N, 24°8'4.67"E), apparently drilled by REMSA (Repsol Exploración Murzuq S.A.), some 530 m NNE of well JA-2 have been investigated for acritarchs and chitinozoans. However, we are not certain that the abandoned well was drilled by REMSA, and therefore we name it UN-REMSA well with UN standing for uncertain. Before starting the chemical processes, each core sample was observed under the binocular microscope in order to collect information on its grain size, petrology, and possible macrofossils. The degree of weathering of the rock sample was also evaluated as oxidation of the rock precludes the preservation of the organic matter (Table 1). This information is useful to interpret low chitinozoan abundances: low abundance in non-weathered and low-energy sediments is mainly caused by environmental conditions and the lack of palynomorphs in weathered or high-energy

deposits, respectively, are due to oxidation of the organic matter, and to non-deposition of the lighter particles such as acritarchs or chitinozoans.

In well JA-2 (Fig. 2), the lowermost core sample at 73.21 m depth is grey shale. Samples from 67.97 to 69.12 m show evidence of weathering (e.g., oxidation of pyrite crystals; brownish micas) in very fine light coloured sandstone and in whitish (altered?) shale. The uppermost processed samples (33.33 m and 46.20 m) also display evidence of weathering (i.e. beige colour of the silty shale and oxidation of the organic matter). This alternation most likely corresponds to the deepest part of the sub-Recent weathering profile developed in many Saharan regions. In the interval 46.60–67.59 m, the lithology is fairly constant and ranges from grey and greenish shale to grey siltstone with micas. A lithological change is noticed between 67.59 and 67.82 m with the occurrence of very fine sandstone. However, for the microfossils, a major change occurs at 67.97 m with a dramatic drop in abundance of the chitinozoans, possibly related to either the oxidation, noticed in the core samples (Table 1), or to temporary emersion (e.g., during the latest Hirnantian−earliest Rhuddanian post-glacial rebound), which permitted the weathering of the older strata. Ground water circulation in a minor fault also might have caused oxidation of the rock and of its organic matter between 67.82 and 69.12 m. Because no biostratigraphical information is available on the underlying strata, it is not possible to favour one or the other of these hypotheses.

The cutting sample SJS0001 from the UN-REMSA well is susceptible to caving. However, because no strong lithological disparity was noticed in the cuttings collected and investigated, the drilled horizon represents likely dark grey silty shale, which is the most common component of the sample.

2.2. Sample preparation

The core material was split into equal parts and prepared separately for acritarch and chitinozoan analysis. For the acritarchs, the samples were treated according to standard palynological preparation methods. A zinc bromide solution (specific gravity 2 g cm^{-3}) was used for separation of organic matter, which was then screened using a 15 μm mesh for washing in order to separate the larger organic-walled microfossils. If necessary, samples were also treated with nitric acid. For chitinozoans, the processing technique developed in the palynological laboratory of Rennes University (see Paris et al., 2012) was adopted. The palynological slides corresponding to the illustrated material on Plates I to V are housed in the CASP Palaeontological Collection in Cambridge, and the palynological slides corresponding to the illustrated material on Plates VI to XII are housed in the collection of Rennes University under the repository numbers IGR 72951 to 72995.

3. Palynological results

Marine acritarchs, leiosphaerids, *Tasmanites*, land-derived plant elements (cryptospores, miospores), and "thread-like structures" possibly related to cyanobacteria or to fungi in association with nearshore chitinozoans, scolecodonts and eurypterid remains are reported in this study (Tables 1 and 2). Large organic "blades" or "sheets", called "biofilm", are also present in the organic residues.

3.1. Marine phytoplankton and land-derived plant element assemblages

3.1.1. Species from well JA-2

151

152 The interval 33.33–69.12 m yielded rich to moderately rich assemblages of acritarchs (Plates I to
153 IV) dominated by *Leiosphaeridia* spp. The presence of *Eupoikilofusa striatifera* at 48.18 m,
154 *Moyeria cabbotti* at 67.82 m and *Leiosphaeridia acerscrabrella* suggest an age no older than
155 Rhuddanian for this interval. Other accessory taxa present in the studied core samples include
156 *Buedingiisphaeridium* sp., *Diexallophasis denticulata*, *Filisphaeridium* sp., *Geron* cf. *gracilis*,
157 *Tunisphaeiridium* sp., *Veryhachium europaeum*, *V. lairdii* and *V. trispinosum* (Table 2).
158 The assemblage is dominated by miospores in the upper part of the interval 46.60–53.07
159 m. Tetrads and other cryptospores are dominant in the interval 48.18–67.82 m. Land-derived
160 spore tetrads are recorded in residues from various depths (see Tables 1 and 3) but mostly in the
161 interval 55.53–62.34 m. Miospores are represented by *Ambitisporites dilutus*,
162 *Archaeozonotriletes chulus* var. *chulus* and trilete spores. Cryptospores are represented by
163 *Dyadospora murusdensa*, *Rugosphaera* sp. and *Tetrahedraletes medinensis*. The presence of
164 these miospores and cryptospores are consistent with an early Silurian (Llandoverian,
165 Rhuddanian) age for the assemblage.
166 A few scolecodonts identified to the generic level (Plate XII, 1−2, 17) are present in the
167 upper part of the core (Table 1). These jaws of marine worms (polychaetes) occur in nearshore
168 as well as in pelagic deposits. Unusual thread-like and branched structures (Plate IX, 1, 6−8;
169 Plate XII, 9, 14, 18) of unknown biological affinities (plant, cyanobacteria or fungi?) are also
170 present in the organic residues (Tables 1 and 3). They are assigned to *Tortotubus protuberans*
171 Johnson, 1985, which seems restricted to latest Ordovician−earliest Llandovery nearshore
172 deposits in northern Gondwana localities (e.g., Chad, Libya, Oman, Saudi Arabia) and North
173 America (Pennsylvania).

One of the peculiar characteristics of the palynological residues of JA-2 is the occurrence of large “blades” or “sheets” (up to 1 mm thick) of amorphous organic matter (Plate IX, 2−5, 10; Plate XII, 15-16). The chitinozoans and other palynomorphs are often adhesively associated with amorphous organic matter (Plate IX, 9; Plate XI, 14−15, 17) as result of which the processes of the Ancyrochitininae break frequently during sorting of the vesicles. These organic sheets are composed of agglomerated minute particles of several μm in length and less than one μm thick (Plate IX, 3 and 10). Pyrite framboids with 10 μm in diameter are recorded, with the exception of a sole specimen of about 500 nm. Under transmitted light microscope, they appear as tiny black spheres in the brownish to yellowish organic sheets. After oxidation with HNO_3, the pyrite is dissolved and the casts of the framboids are visible (Plate IX, 5 and 10). The organic sheets are here called “biofilms”, produced by algae or by bacteria. The organic matter in the northern Gondwana “hot shale” has a similar structure with minute “flakes” of organic particles adhesively clumped with the organic-walled microfossils. However, in the JA-2 well samples, the AOM is concentrated in films coating the bedding plane, whereas in the classical “hot shale” this organic matter is a major component of the sediment (up to 30% in some cases). This organic matter may represent remnants of algae.

3.1.2. Species from the UN-REMSA well

Cutting samples (SJS0001) from the UN-REMSA well, located some 530 m NNE of JA-2, yielded sparse acritarchs including *Leiosphaeridia* sp. and *Eupoikilofusa striatifera* (Table 2). Land-derived palynomorphs include *Ambitisporites dilutus* and a spore tetrad along with *Tortotubus protuberance* (Table 3). These taxa are also present in the core samples from JA-2.

197 The sediment was deposited in a shallow marine environment. The sample is rich in AOM with
198 TAI <3, suggesting an immature kerogen with poor source potential.
199
200 *3.2. Chitinozoan assemblages*
201
202 *3.2.1. Species from well JA-2*
203
204 Most of the processed samples, except the two uppermost (33.33 and 46.20 m) and the
205 lowermost interval (67.97–73.21 m), which are likely to be affected by oxidation (see above),
206 yield well-preserved chitinozoan assemblages with transparent and brownish to yellowish
207 vesicles (Plates X–XI). They are poorly diversified and frequently monospecific assemblages
208 (see Fig. 4). However, the chitinozoan abundance is fairly high as it exceeds 100 specimens per
209 gram of rock in half of the productive samples, and even reaches 430 specimens per gram of
210 rock at 57.58 m (Fig. 2; Table 1). In the other samples, the chitinozoan abundance ranges around
211 60 to 80 specimens per gram of rock, except at 60.23 and 62.34 m depth where the abundance
212 drops significantly with 23 and 5 specimens respectively per gram of rock. It is worth noting that
213 eurypterid remains (Plate XII, 3−6) and *Tasmanites tzadiensis* Le Hérissé (in Le Hérissé et al.,
214 2013) (Plate XII, 7−8, 11−13) are associated in these two samples (Table 1). This suggests
215 shallower environments with prominent agitation in which the sediment (siltstones with large
216 micas) becomes more mobile so that a selective sorting of the lighter particles occurs.
217 All the investigated samples, except those from 67.59–67.97 and 73.21 m, are dominated
218 by a single species, *Euconochitina moussegoudaensis* Paris (in Le Hérissé et al., 2013), which
219 represents 95 to 100 % of the recovered assemblages (Fig. 4). This species dominates also the
220 chitinozoan assemblages recorded in the Moussegouda shallow core in NW Chad (Le Hérissé et

al., 2013) from grey silty shale intervals as in well JA-2. Furthermore, it has been described from the Late Ordovician of Eastern Alborz in northern Iran (Ghavidel-Syooki, 2008).

E. moussegoudaensis is a simple form (see diagnosis and description by F. Paris in Le Hérissé et al. 2013 and Plate VI, 4a−b, 8a−b; Plate VII, 5; Plate VIII, 3a-b, 4, 5a-b; Plate X, 1, 5−8, 10, 12, 14−16, 18; Plate XI, 16, 18-20). Its conical chamber has gently tapering flanks and a flat to slightly convex bottom, which may be variously affected during the flattening (folded inside or outside the chamber giving a more or less sharp aspect to the margin; see Plate X). No mucron or basal scar has been observed on the available material. The sub-cylindrical neck represents one third or less of the vesicle length, which ranges from ca. 100 to 200 μm. The weak flexure is located at the base of prosome, near the junction of the rica on the chamber inner wall (only visible on the transmitted light photos; Plate X). The wall surface is practically smooth, but at high magnification, SEM observation reveals very tiny granules (Plate VI, 4b), which are better expressed on, or near the margin (Plate VI, 8b). This species has no highly distinctive features (i.e., ornamentation). However, it can be identified on large populations allowing the appraisal of the intraspecific morphological variations.

During the present study, elongate specimens sharing most of the characters of *E. moussegoudaensis* Paris have been observed together with the typical form. These slender individuals are tentatively separated from the main morphotype. They are referred to as *Euconochitina* cf. *moussegoudaensis* Paris in Fig. 4 and on Plate X, 2−3, 9, 11, 19−20 and Plate XI, 3, 5, 11. The vesicle length exceeds 200 μm and may reach 230 μm. A weak constriction is visible at a short distance above the margin (e.g., Plate X, 2, 19−20). It is not clear yet if these elongate and slender vesicles correspond to the end forms within a polymorphic species or if they represent a different species, with a stratigraphical range partly overlapping the total range of *E. moussegoudaensis* Paris.

Besides the dominating *E. moussegoudaensis* Paris are subordinate species restricted to one or two samples. *Calpichitina* sp. (Plate X, 13) is restricted to one specimen recorded at 66.85 m depth. The membranous remains visible on the margin are most likely residues of the biofilm somehow glue the vesicle, and not part of a carina as in *Pterochitina deichaii*.

Two species of *Spinachitina* − *S. oulebsiri* Paris et al. (2000) and *Spinachitina verniersi* Vandenbroucke in Vandenbroucke et al. (2009) − are recorded in well JA-2. For the former, the most abundant population is from 67.59 m (Fig. 4) but a few individuals are also recorded at 67.21 and 67.40 m. *Spinachitina oulebsiri* (Plate VII, 1a−c, 3a−b, 4a−b, 6, 8 and 9a−c; Plate XI, 1, 6−10) has a conical chamber and a rather short sub-cylindrical neck (about one third of the vesicle length) ended with a denticulate aperture (Plate VII, 9c). The margin bears a crown of ca. 20 slender conical spines of up to 6 μm length (Plate VII, 1b, 3b, 4b and 9b). Butcher (2009, p. 600) included *S. oulebsiri* in the synonymy list of *S. fragilis*, which is the index species for the first Silurian chitinozoan biozone (Verniers et al., 1995). Even if they have close silhouettes, we do not consider the two species as synonyms. This is in agreement with Vandenbroucke et al. (2009) who reported *S. oulebsiri* from South Africa (see below). Indeed, *S. oulebsiri* has not the conspicuous shoulder of the specimens Butcher assigned to *S. fragilis* from depth 42.50 m in BG-14 in Jordan. Moreover, the populations of *S. oulebsiri* known in various localities from Algeria (Paris et al., 2000; F. Paris, unpublished data) and South Africa (Vandenbroucke et al., 2009) do not include large specimens (>250 μm) as known in *S. fragilis*. Based on the discussion below, *S. oulebsiri* ranges from the late Hirnantian to possibly earliest Rhuddanian (see Fig. 5). Poorly preserved individuals from 62.34 m are tentatively referred to *S.* sp. aff. *oulebsiri*.

In well JA-2 (Fig. 4), *Spinachitina verniersi* Vandenbroucke (in Vandenbroucke et al., 2009) (Plate VI, 3a−b; Plate VII, 2a−b) is fairly abundant at 67.59 m and is represented by a few individuals at 65.74 m (see Fig. 4). This species, first described from the Soom Shale in South

269 Africa (Vandenbroucke et al., 2009), has a vesicle very close to that of *S. oulebsiri* and even to
270 that of *E. moussegoudaensis* Paris. However, it is clearly distinguished from *S. oulebsiri* by the
271 design of the crown of ornaments running on its margin (more densely spaced and irregular
272 granules or blunt spines) (see Plate VII, 2a). Closely related specimens (*S.* cf. *verniersi*; Plate XI,
273 4) or more questionable individuals referred to as ?*S. verniersi* (Plate VI, 1a−b, 2a-b, 6a−b,
274 7a−b; Plate VII, 7) due to a poor preservation of the crown on the margin are scattered from
275 55.53 m depth to 67.82 m depth in well JA-2 (Fig. 4). *S. verniersi* does not benefit yet from an
276 accurate independent calibration by means of graptolites. However, in South Africa its FAD
277 (First Appearance Datum) is in the Soom Shale Formation, i.e. just above the last Hirnantian
278 glacial deposits (see discussion in Vandenbroucke et al., 2009). In Algeria, it also coexists with
279 *S. oulebsiri* in the M'Kratta Formation above the Hirnantian diamictites of the Hassi el Hadjar
280 Formation (see discussion in Paris et al., 2000). *S. verniersi* is also recorded in the cuttings from
281 the UN-REMSA well (Plate VIII, 6a−c, 9a−b, 10a−b) where it occurs in association with *E.*
282 *moussegoudaensis* Paris.
283 The Ancyrochitininae, abundant at 67.82 m depth, are present sporadically. *Plectochitina*
284 sp. (Fig. 4) is another form kept in open nomenclature because of its poor preservation. They
285 belong possibly to *Plectochitina* cf. *longispina* (Achab, 1978), which is the dominating species
286 at 67.82 m depth (Plate VI, 5, 10; Plate XI, 13−15, 17). These specimens are assigned to
287 *Plectochitina* rather than to *Ancyrochitina* because of the cell-like structure of their long
288 processes (Plate X, 15 and 17). The individuals recorded at 67.82 m depth are rather small, e.g.
289 vesicle length ranging from 100 to 120 μm. The length of the processes is about 40 to 60 μm.
290 These values are very close to the measurements of *Ancyrochitina longispina* described by
291 Achab (1978) in the Ellis Bay Formation of Anticosti Island, Eastern Canada. The Libyan and
292 the Canadian specimens have processes with similar branching. The main difference between the

two populations is the less developed branching of the Libyan individuals (2 times branching as a maximum). According to Achab (1978) and Soufiane and Achab (2000), *A. longispina* is restricted to the lower member of the Ellis Bay Formation assigned to the early Hirnantian (i.e. *extraordinarius* graptolite Zone) by Melchin (2008). Recently, Butcher (2009) published a form he called *Ancyrochitina* sp. C, which displays most of the features of the individuals identified here as *Plectochitina* cf. *longispina*, i.e. short vesicle. However, the form illustrated by Butcher (2009) from BG-14 in Jordan is from the upper *ascensus−acuminatus* Biozone (early Rhuddanian). Obviously, there is an urgent need of clarification of the Ancyrochitininae close to the Ordovician−Silurian boundary, especially the forms with long processes.

3.2.2. Species from the UN-REMSA well

The composition of its organic residue is very similar to most of the residues recovered from well JA-2. It includes fairly numerous chitinozoans, scolecodonts and biofilms. However, neither "thread-like structures", nor "*Tasmanites* with nodules" (i.e. *Tasmanites tzadiensis* Le Hérissé in Le Hérissé et al. 2013) have been observed in this residue.

The cuttings from the UN-REMSA well (sample SJS0001) yield a chitinozoan assemblage very close to that observed in well JA-2. *Euconochitina moussegoudaensis* Paris (Plate VIII, 2a−b; 4, 5a−b) is again the dominant species. It is accompanied by rare *Cyathochitina caputoi* Da Costa, 1971 (Plate VIII, 1). *C. caputoi* (the thick carina form), which is usually very abundant close to the Ordovician−Silurian boundary is not observed in well JA-2. A few *Spinachitina verniersi* (Plate VIII, 6a−c, 9a−b, 10a−b) and damaged Ancyrochitininae (Plate VIII, 7−8) (broken processes do not allow any specific assignment) are also present in this assemblage and are assigned to the latest Hirnantian−earliest Rhuddanian (see Fig. 5).

317

318 *3.3. Kerogen analysis and thermal maturity*

319

320 Visual kerogen analysis using transmitted light microscopy was carried out on 23 samples from
321 the interval 33.33–73.21 m (Table 4). The analysis results are summarised in Figure 2. The
322 interval 33.33–46.20 m is completely dominated by semi-structured (Type 3), vitrinite-like
323 material. No acritarchs or miospores were recorded in this interval. The interval 46.60–67.40 m
324 is generally dominated by AOM (Type 1) but semi-structured, vitrinite-like material continues to
325 show its presence throughout the interval (see Appendix A). A high number of acritarchs along
326 with miospores/cryptospores are also documented. *Leiospheridia* spp. dominate in numbers, and
327 spiny acanthomorph acritarchs are low in numbers. The interval 67.59–73.21 m, with the
328 exception of core at 69.92 m depth, in which AOM dominates, is abundant in semi-structured,
329 vitrinite-like material.

330 Based on the colour of the miospores, the thermal alteration index (TAI) (Staplin, 1969)
331 is less than 3, indicating an immature palynofacies for oil generation. Acritarchs and
332 cryptospores are consistently pale and light yellow in colour, which probably indicates a lack of
333 thermal alteration. Chitinozoan reflectance yielded R_{ch} values of about 0.6% (Table 5) which
334 equals vitrinite reflectance (R_v) values of about 0.4% when using the equation of Tricker et al.
335 (1992). Sediment with R_v of 0.4% is immature for oil generation, supporting the TAI
336 interpretation.

337

338 **4. Biostratigraphy, palaeoecology and regional correlation**

339

340 *4.1. Marine phytoplankton and land-derived plant element assemblages*

341

342 The acritarchs assemblage is dominated by thin-walled *Leiosphaeridia* spp. often in clusters.
343 Dorning (1981) found dominance of thin-walled leiosphaerids in the shallow marine Silurian
344 (Ludlovian) sequence of the Welsh Borderland. The presence of land-derived vitrinite-like
345 macerals and miospores–cryptospores is also indicative of a marginal marine (nearshore)
346 depositional environment for the entire sequence of the studied well JA-2, although the interval
347 33.33–60.23 m does seem much closer to land with the dominance of land-derived plant
348 remains.

349 In the late Silurian of the Ghadamis Basin, Al-Ameri (1983) erected six distinct types of
350 palynofacies of which four contained acritarchs indicating increasing distance from the
351 shoreline. Hill and Molyneux (1988) recognised two Llandoverian palynofacies assemblages in
352 NE Libya. Their southern assemblage located in southern Cyrenaica, north of the present study
353 area, was also dominated by leiosphaerids. Hill and Molyneux (1988) consider their acritarch
354 assemblage comparable most closely to Palynofacies 3 of Al-Ameri (1983), which is interpreted
355 as inner neritic.

356 The studied assemblage is also comparable to the land-derived palynoflora (miospores–
357 cryptospores and organic structures) of early Silurian (Rhuddanian) age from the Tuscarora
358 Formation in central Pennsylvania, USA (Johnson, 1985). Based on these comparisons the
359 present assemblage was probably deposited closer to the shoreline.

360

361 *4.1.1. Libya*

362

363 Acritarch assemblages recorded in well JA-2 are similar to those from other basins in North
364 Africa, the Middle East, and North America (Fig. 3).

365

366 Kufra Basin

367

368 Grignani et al. (1991) established a zonation of the early Silurian Assemblage C based on the
369 chitinozoan *Ancyrochitina ancyrea*. However, the authors reported no early Silurian acritarchs.
370 The marker acritarchs such as *Villosacapsula irrorata*, *V. setosapellicula* and *Veryhachium*
371 *subglobosum* restricted to the Late Ordovician (Caradoc–Ashgill) were reported by Grignani et
372 al. (1991) and by Thusu et al. (2007) from cutting samples from Jebel Dalma.

373

374 Murzuq Basin

375

376 Paris et al. (2012) reported an early Llandovery palynomorph assemblage from well CDEG-2a in
377 Dor el Gussa and recorded palynomorph species which are also present in the present study
378 including *Buedingiisphaeridium* sp., *Diexallophasis denticulate*, *Eupoikilofusa striatifera*,
379 *Leiofusa estrecha*, *Veryhachium. europaeum*, *V. trispinosum*, *Dyodospora murusdensa* and
380 *Tetrahedraletes medinensis*.

381

382 Ghadamis Basin

383

384 Richardson and Ioannides (1973) reported a rich assemblage of Silurian acritarchs from two
385 wells, C1-34 and B2-34, from the Akakus and Tanezzuft formations in the Ghadamis Basin. The
386 recorded species in common with the present assemblage include *Eupoikilofusa striatifera*,
387 *Veryhachium trispinosum*, *Diexallophasis denticulata*, *Leiosphaeridia acerscabrella*, *Leiofusa*
388 *estrecha*, *Geron* cf. *gracilis*, *Tetrahedraletes medinensis* and *Dyadospora murusdensa*.

Northeast Libya, Cyrenaica

Hill et al. (1985), Hill and Molyneux (1988) and Richardson (1988) recorded early Silurian (Llandoverian) acritarchs from the Cyrenaica Platform. Several species recorded from Cyrenaica are common with the present assemblage and include *Eupoikilofusa striatifera*, *Diexallophasis denticulata*, *Tunisphaeridium* sp., and *Buedingiisphaeridium* sp..

4.1.2. Chad

Le Hérissé et al. (2013) reported latest Ordovician–earliest Silurian palynological assemblages from the Moussegouda shallow borehole (21°40'N, 18°36'E) drilled in the Erdi Basin, northern Chad in the early 1960s. The Erdi Basin and the Mourdi Basin in northwest Sudan are considered to be the southern extensions of the Kufra Basin to the north in Libya.

The presence of several stratigraphically restricted acritarchs reported from core 9 (220–221A m) from the Moussegouda borehole such as *Neoveryhachium* sp. A, *Veryhachium subglobosum* and *Villosacapsula setosapellicula* clearly support an age no younger than Late Ashgill for this interval. *V. subglobosum* and *V. setosapellicula* were also recorded by Grignani et al. (1991) in their assemblage 'B' in the Kufra Basin. None of these species were recorded in our study. The absence (except in the basal part) of these species together with the common presence of *Tasmanites tzadiaensis* Le Hérissé et al. (2013) and many reported acritarchs and chitinozoans, cryptospores and miospores in cores 8–2 from the Moussegouda well in Chad and those in well JA-2 in Libya support their close chronostratigraphic and ecological similarities.

The oldest recorded early Silurian (late Rhuddanian) local Biozone LI1 was first reported by Hill and Molyneaux (1988) from an exploratory well (E1-81) in Cyrenaica northeast Libya and recently by Paris et al. (2012) from a shallow borehole (CDEG-2) in Dor el Gussa, eastern Murzuq Basin. In both areas, the incoming of marker species *Diexallophasis caperoradiola*, *Multiplicisphaeridium fisherii* and *Oppilatala eoplanktonica* clearly support a Late Rhuddanian age. None of these species were either recorded in Le Hérissé et al. (2013) in the Moussegouda well or in the present study in the JA-2 well. Based on these observations, it is inferred that the post-Ashgillian interval in the Moussegouda well (cores 8–2) and in well JA-2 may represent a time interval between the latest Ordovician and earliest Silurian. However, the presence of *Geron cf. gracilis*, *Moyeria cabotii, Tunisphaeridium* sp., *Ambitisporites dilutus* and *Archaeozonotriletes chulus* var. *chulus* and *Tortotubus protuberans* in well JA-2 does appear to demonstrate an early Silurian age for the JA-2 assemblage. Furthermore, we cannot rule out the extension of the well JA-2 sequence to the post-glacial latest Hirnantian because the post-glacial latest Hirnantian acritarch and miospore assemblage is poorly documented in North Africa. The palynomorph content in both wells is supportive of a marginal marine (nearshore) environment and may represent a post-glacial pre-Tanezzuft Formation (sensu stricto) sedimentary sequence.

4.1.3. Algeria

Jardine et al. (1974) recorded early Silurian acritarch assemblages from the Algerian Sahara and established Palynozones G1 and G2. Species common to the Algerian and present assemblage include *Diexallophasis denticulate*, *Eupoikilofusa striatifera*, *Leiofusa estrecha* and *Veryhachium trispinosum*.

436

437 *4.1.4. Saudi Arabia*

438

439 Le Hérissé et al. (1995) recorded early Silurian (Llandovery, Rhuddanian and Aeronian)
440 palynomorphs assemblage from Saudi Arabia. They recorded *Buedingiisphaeridium* sp., *D.*
441 *denticulata*, *E. striatifera*, *Filisphaeridium* sp., *Geron* sp., *Moyeria cabottii* and *Tunisphaeridium*
442 sp..

443

444 *4.1.5. Jordan*

445

446 Keegan et al. (1990) recorded early Silurian palynomorphs from two exploration wells of the
447 Hashemite Kingdom of Jordan. The morphotypes *Geron gracilis*, *D. murusdensa*, *Ambitisporites*
448 *dilutus* and *Archaeozonotriletes chulus* var. *chulus* are present in zone JS-3 (early Llandoverian)
449 of Jordan and are also recorded in the present study.

450

451 *4.1.6. North America*

452

453 The studied assemblage in well JA-2 is closely comparable with the early Silurian (Rhuddanian)
454 assemblage from the Tuscarora Formation in central Pennsylvania, USA (Johnson, 1985).
455 Common species include *L. acerscabrella*, *T. mediensis*, *A. dilutus*, *Rugosphaera* cf.
456 *tuscarorensis* and *Tortotubus protuberans*.

457

458 *4.2. Chitinozoan assemblages*

459

460 Available data on chitinozoans from the Ordovician−Silurian boundary increased significantly
461 during the last ten years with the work of Bourahrouh (2002) (data on Algeria, Morocco, western
462 France and Czech Republic) and the papers of Vandenbroucke et al. (2009) on the chitinozoans
463 from the Soom Shale of South Africa, and of Butcher (2009) on those of the Mudawwara Shale
464 Formation in Jordan. A few new species are erected in these contributions. However, an
465 extensive taxonomical study of many undescribed new forms from the Late Ordovician−early
466 Silurian of northern Gondwana regions, based on large populations, is now urgently needed.
467 Independent biostratigraphical control by means of graptolites is now available for some
468 chitinozoan-bearing sections, e.g. Nseirat section, Mauritania (Underwood et al., 1998; Legrand,
469 2009), Jordan (Lüning et al., 2006; Loydell, 2007, 2012), Les Fresnaies section, southern
470 Brittany, France (Piçarra et al., 2009), and Hlasna Treban, Czech Republic (Štorch, 1996; Štorch
471 and Loydell, 1996). All these data now allow a reassessment of the chitinozoan assemblages
472 formerly described in NE Libya by Molyneux and Paris (1985) and by Paris (1988).
473 The occurrence of chitinozoans throughout the penetrated sequence in JA-2 (except the barren
474 lowermost samples; see above) clearly indicates a marine deposit. The rather low diversity of the
475 recorded assemblages, in spite of high abundance (up to 415 specimens per gram of rock), is
476 compatible with deposition in a rather proximal setting to the shoreline. This is consistent also
477 with the occurrence of land-derived cryptospores and miospores in association with vitrinite-like
478 organic matter in the residues. The presence of eurypterids (Plate XII, 3−6) is also in favour of
479 environments not very far from the shoreline as these animals are regarded as nearshore (e.g.,
480 Jones and Kjellesvig-Waering, 1985), and in some cases occasionally terrestrial organisms
481 (especially in the late Silurian) (e.g., Braddy, 2001). The occurrence of *Tortotubus protuberans*
482 (Plate XII, 9, 14, 18) provides an additional indication of deposition fairly close to the shoreline,

as this enigmatic microfossil is usually reported from shallow to terrestrial environments at the Ordovician−Silurian boundary (e.g., Le Hérissé et al., 2013).

4.3. Ordovician−Silurian boundary

The definition of the base of the Silurian, and thus of the Rhuddanian Stage is a critical point for the calibration of the latest Ordovician−earliest Silurian chitinozoan assemblages. The Ordovician−Silurian boundary first moved from its historical position at the base of the *persculptus* Biozone, to the base of the succeeding *acuminatus* Biozone, with the GSSP of the base of the Silurian defined at Dob's Linn in Scotland (see Williams and Ingham, 1989). The basal Silurian *acuminatus* Biozone at Dob's Linn was subsequently subdivided into a lower *Akidograptus ascensus* Biozone and a higher, more restricted *Parakidograptus acuminatus* Biozone (Melchin and Williams, 2000). As a consequence, the base of the Silurian (base of the Rhuddanian) is now defined by the first appearance of *A. ascensus*. This definition was ratified by the International Subcomission on Silurian Stratigraphy (2007). Moreover, recent revisions of graptolites from the *ascensus–acuminatus* Biozone (e.g., Loydell, 2007, 2012, and references therein) confirm the three-fold divisions of this biozone by Štorch (1996) into lower, middle and upper subzones. In this scheme (see Loydell, 2007, p. 10), *A. ascensus* ranges in the lower and the middle subzones. All these successive changes had consequences on the accurate dating of the chitinozoan biozones around the Ordovician−Silurian boundary, as there are no direct ties with the GSSP at Dob's Linn (no workable chitinozoan assemblages are available yet; see Verniers and Vandenbroucke, 2006). Delabroye and Vecoli (2010) briefly reviewed the biostratigraphical inconsistencies persisting in the main diagnostic fossil groups close to the Ordovician–Silurian boundary.

507

508 *4.4. Chronostratigraphical calibration of the Hirnantian and Rhuddanian chitinozoan biozones*

509

510 Continuous chitinozoan-bearing strata of latest Ordovician to early Silurian age, i.e. not
511 disturbed by Hirnantian glacial events, are very rare in northern Gondwana regions (including
512 peri-Gondwana Europe, sensu Štorch, 1996). At a few localities this boundary can be located
513 with the greatest precision, for example, in the Nseirat section in the Hodh area (Mauritania),
514 which yielded associated abundant graptolites (Underwood et al., 1998; Legrand, 2009) and
515 chitinozoans (Paris et al., 1998; F. Paris, unpublished data). The Hlasna Treban section in the
516 Prague Basin (Czech Republic) also yielded well studied graptolites (Štorch, 1996; Štorch and
517 Loydell, 1996) and chitinozoan data (Dufka and Fatka, 1993; Bourahrouh, 2002). Another
518 section is at les Fresnaies, Ancenis Basin, western France, where Hirnantian chitinozoan-bearing
519 diamictites (Bourahrouh, 2002; F. Paris, unpublished data) are overlain by Rhuddanian black
520 shale with associated graptolites and chitinozoans (Bourahrouh, 2002; Piçarra et al., 2002;
521 Piçarra et al., 2009; F. Paris, unpublished data). The Ordovician–Silurian boundary can also be
522 located with the greatest precision in well BG-14 in southern Jordan where graptolites (Loydell,
523 2007) and chitinozoan (Butcher, 2009) have been studied. In southern Saudi Arabia chitinozoans
524 occur in the MKSR-1 well, just below and within graptolite-bearing black shale assigned to the
525 early Rhuddanian (Paris et al., 1995). Other important controls should be obtained from the
526 graptolite-bearing sequence in the E1-NC174 core in the Murzuq Basin (Libya) as chitinozoans
527 are also reported (Butcher, 2012) with abundant early Rhuddanian graptolites (Loydell, 2012).
528 The concurrent ranges of the chitinozoans and graptolites in these sections are used here for
529 more precise dating of numerous previously published chitinozoan assemblages close to the
530 Ordovician−Silurian boundary (Fig. 5).

In the present study on core samples from JA-2, the comparison focuses chiefly on the chitinozoan data available for Libya, with a particular attention paid to the chitinozoan assemblages from the Kufra Basin, e.g. KW-2 core-drill (Grignani et al., 1991; Le Hérissé et al., 2013; F. Paris, unpublished data), cores from wells A1-NC43 and B1-NC43 (Grignani et al., 1991), and cuttings from H6000 and W5174 (Paris et al., 2008) (Fig. 5). Correlation is also proposed with other Libyan regions, e.g. well CDEG-2a in the eastern Murzuq Basin (Paris et al., 2012). The Silurian chitinozoans of Al-Ameri (1989) from Western Libya, however, are not discussed here as they correspond to assemblages younger than the material recovered from the sub-surface of the Kufra Basin. Older data from Cyrenaica (Molyneux and Paris, 1985; Paris, 1988), which did not benefit from an independent calibration in terms of graptolite biozones, can now be updated. The correlations are extended to cores in other countries, e.g. Moussegouda, northern Chad (Le Hérissé et al., 2004, 2013).

In Moussegouda, the occurrence of glacio-marine deposits with typical Late Ordovician chitinozoans and acritarchs ca. 15 m below the first *E. moussegoudaensis* chitinozoan assemblage must be stressed, as this demonstrates that the *E. moussegoudaensis* dominated assemblage is clearly post-glacial. In well KW-2, *E. moussegoudaensis* occurs in the shale referred to the Tanezzuft Formation (Le Hérissé et al., 2013). Below 54 m of this Tanezzuft Formation shale, the well penetrated sandstone of the Mamuniyat Formation for 7 m. No chitinozoans are reported from this sandy member but typical latest Ordovician chitinozoan assemblages are present in the neighbouring wells of A1-NC43 (core 3, Mamuniyat Formation) and B1-NC43 (core 5; but supposed to belong to the Tanezzuft Formation in Grignani et al., 1991). The lithostratigraphic position of the latter core sample, however, is confusing (see discussion in Grignani et al., 1991, p. 1163). No graptolites have been identified in JA-2 or in Moussegouda, but Grignani et al. (1991) reported "*Climacograptus medius*" (now

555 *Normalograptus medius*) in the KW-2 cores. If the identification is correct, this means that the
556 corresponding samples can be of late Hirnantian as well as of Rhuddanian age as this species
557 ranges across the Ordovician−Silurian boundary (see Loydell, 2007, text in fig. 6). In areas of
558 JA-2 and KW-2, we do not have unweathered material from the overlying formations. In
559 Moussegouda, the shale sequence with the *moussegoudaensis* chitinozoan assemblage is directly
560 overlain by barren white sandstone referred to the Akakus Formation. No biostratigraphical data
561 are available in the Silurian part of A1-NC43 and B1-NC43. Consequently, the top of the
562 *moussegoudaensis* assemblage is not constrained in the Kufra Basin, even when this structure is
563 extended to northern Chad.
564 The ranges of *S. oulebsiri* and *S. verniersi*, two taxa represented in the *moussegoudaensis*
565 assemblage, have been used to better constrain its chronostratigraphic assignment. *S. oulebsiri*
566 ranges in late Hirnantian post-glacial deposits, especially in the Nseirat section (Mauritania),
567 where it coexists briefly with *Belonechitina pseudarabiensis* and *Cyathochitina caputoi*. The
568 latter have their Last Appearance Datum (LAD) higher up in the section in the well-dated upper
569 *ascensus−acuminatus* Biozone of early Rhuddanian age. The lower part of the Nseirat section
570 (with *S. oulebsiri*) yields abundant *Normalograptus* graptolites attributed to the *persculptus*
571 Biozone (Underwood et al., 1998), i.e. of late Hirnantian age. However, the specific assignment
572 of these *Normalograptus* have been recently contested by Loydell (2007) who rejected the
573 specimens of *N. persculptus* illustrated by Underwood et al. (1998) from his well-documented
574 synonymy list for *N. persculptus* (Loydell, 2007, p. 43).
575 Because the durations of the related glacial events are significantly shorter (ca. 10 ky)
576 than the range of the recorded chitinozoan species (ca. 1 Ma or more), the Hirnantian glacial
577 climax can be regarded as isochronous at the scale of the northern Gondwana chitinozoan
578 biozonations. Indeed, several typical Late Katian species, e.g. *Calpichitina lenticularis*,

579 *Armoricochitina nigerica*, *Desmochitina* gr. *minor*, *Lagenochitina baltica*, *L. prussica* (see Paris
580 et al., 2000, and references therein) range through the Hirnantian, up to the end of the main
581 melting phase of the ice cap, in the latest Hirnantian. Fortunately, some taxa have a more
582 restricted range and proved to be helpful for subdividing the latest Ordovician. *Tanuchitina*
583 *elongata*, the index species of the next to last Ordovician chitinozoan biozone (Paris, 1990) has
584 its FAD before the first drastic sea level fall characterising the beginning of the Hirnantian
585 glacial climax. This FAD is located just above the base of the Hirnantian as documented in the
586 Anti-Atlas, Morocco (Loi et al., 2010) and in the Prague Basin by Bourahrouh (2002) where *T.*
587 *elongata* is recorded in association with *Normalograptus osjuensis*. The latter graptolite is
588 regarded as slightly preceding the FAD of *N. extraordinarius*, the index graptolite of the base of
589 the "new" Hirnantian stage (see Chen et al., 2000, 2006) and thus *T. elongata* begins also just
590 below the base of the Hirnantian. The species is recorded up to the uppermost Kosov Formation
591 (Hirnantian) in the Prague Basin (Bourahrouh, 2002) where *N. persculptus* is present (Štorch and
592 Loydell, 1996). The total range of *T. elongata* is therefore latest Katian−late Hirnantian.
593 At present, *Spinachitina oulebsiri* Biozone is the last Ordovician chitinozoan biozone in
594 the northern Gondwana biozonation (Webby et al., 2004). This species coexists for a time with
595 the last typical Ordovician chitinozoan species (see above) and thus its lower part is late
596 Hirnantian in age. The LAD of *S. oulebsiri* is documented in the lower part of the Nseirat section
597 (up to MSE-10) where it is associated with other chitinozoans with dominating *Cyathochitina*
598 *caputoi* and rare *Belonechitina pseudarabiensis*. This chitinozoan assemblage coexists with
599 numerous *Normalograptus* assigned to *N. persculptus* by Underwood et al. (1998), but not
600 included in the synonymy list of this species proposed by Loydell (2007). Additional
601 information is available from the MKSR-1 well (southern Saudi Arabia) where *S. oulebsiri* is
602 restricted to strata below the 'hot shale' horizon yielding numerous *C. caputoi* associated with

603 graptolites of the *acuminatus* Zone (Paris et al., 1995, and discussion in Paris et al., 2013).
604 According to the graptolites, *S. oulebsiri* may therefore extend into the uppermost Hirnantian or
605 the lowermost Rhuddanian. Based on the synonymy proposed by Vandenbroucke et al. (2009),
606 *S. oulebsiri* is present in the United Kingdom (Vandenbroucke et al., 2005; Vandenbroucke,
607 2008). This species is reported from other localities devoid of accurate independent age control,
608 e.g. Soom Shale in South Africa (Vandenbroucke et al., 2009), several wells in Algeria,
609 including Nl-2 (Paris et al., 2000), and sections in Argentina (De La Puente, 2009). It is also
610 present in JA-2 in SE Libya (see Fig. 4). In these localities, it is worth noting that *S. oulebsiri*
611 without the typical Late Ordovician species but associated with *S. verniersi*, occurs in post-
612 glacial deposits. This confirms that the climax of the Late Ordovician glaciation ended within the
613 *persculptus* Biozone.
614 Slightly higher in the Nseirat section (from NSE-11 to NSE-18) *B. pseudarabiensis* and
615 *C. caputoi* dominate the chitinozoan assemblages. They are associated with *S. debbajae* in strata
616 referred to the lower-middle subzone of the *ascensus−acuminatus* Biozone based on its
617 graptolite content (Underwood et al., 1998) and on the comments provided by Loydell (2007).
618 From NSE-18 onward, *B. pseudarabiensis* is associated with *S. fragilis* (morphotype with a
619 shoulder) and with graptolites of the *ascensus−acuminatus* Biozone from NSE-18. A similar
620 situation occurs also in Jordan (Butcher, 2009), in BG-14 core sample at 42.5 m depth assigned
621 by Loydell (2007) to the upper subzone *ascensus−acuminatus* Biozone. In the Les Fesnaies
622 section, western France (Bourahrouh, 2002; F. Paris, unpublished data), and in Hlasna Treban
623 section, Czech Republic (Dufka and Fatka, 1993; Bourahrouh, 2002) identical *S. fragilis*
624 specimens are associated with graptolites of the *ascensus−acuminatus* graptolite Biozone
625 described respectively by Piçarra et al. (2009) and by Štorch (1996).

In Libya, in the Murzuq Basin, a chitinozoan assemblage similar to that of the upper middle part of the Nseirat section, i.e. *S. fragilis* "with shoulder" associated with Ancyrochitininae specimens with long branched processes (provisionally identified as *A.* cf. *ramosaspina*) is reported from the interval 47.48–50.64 m (core 20 to core 23) in well CDGE-2a (see Paris et al., 2012). In the Kufra Basin, in cuttings samples (W5174 and H6000) abundant *B. pseudarabiensis* coexist with Ancyrochitininae (long processes branched at their distal end, provisionally referred to as *A. gr. ancyrea* in Paris et al. (2008a). Based on the chitinozoan data from Jordan newly published by Butcher (2009) on BG-14 core samples accurately dated by graptolites (Loydell, 2007), the two Kufra assemblages from W5174 and H6000 can be correlated with the upper part of the *ascensus−acuminatus* graptolite Biozone of Jordan, where *S. fragilis* is no longer present (Butcher, 2009, text in fig. 7).

The re-evaluation of previous chitinozoans from Libya enables more accurate dates for assemblages. For instance, the chitinozoans recovered from JI-81A, E1-81 and A1-81 wells of southern Cyrenaica (Molyneux and Paris, 1985; Hill et al., 1985; Paris, 1988) are updated with regards to the range of the chitinozoan key species selected in the present report (Fig. 5). In well J1-81A, cuttings from 12150 ft to 13240 ft, yielded caved specimens of *S. debbajae*, *S. oulebsiri*, and *E. moussegoudaensis* mixed with well-characterised in-situ Hirnantian species. This means that below the Middle Devonian, and above the Upper Ordovician strata, this well penetrated Rhuddanian deposits (see stratigraphical interpretation on Figure 5). In well E1-81, the Ordovician−Silurian beds seem rather better developed, as there is a large interval of ca. 100 m separating core 4 of early Rhuddanian age (abundant *Sphaerochitina solitudina* consistent with the upper subzone of the *ascensus−accuminatus* Biozone), from core 5 of Hirnantian age (*elongata* Biozone) (Fig. 5).

5. Conclusions

The chitinozoan assemblages recovered from the 35 m thick shaly to silty sequence in well JA-2 are characterised by dominant *Euconochitina moussegoudaensis* and by the sporadic, but stratigraphically important presence of *Spinachitina oulebsiri*, *S. verniersi*, and highly branched Angochitininae. These characteristics are shared by the chitinozoan assemblages observed in the ca. 100 m thick shale dominated sequence penetrated by the Moussegouda well (northern Chad; Le Hérissé et al., 2013) and in the 4 core samples analysed previously in the KW-2 shallow core (Kufra Basin, Libya; see Grignani et al., 1991; F. Paris in Le Hérissé et al., 2013). The Moussegouda area is geologically regarded as part of the Kufra Basin (see e.g., Lüning et al., 2006) and therefore, the more complete data available on this well can be of some help in interpreting the core from well JA-2 and cuttings from the UN-REMSA well where the overlying and underlying strata are not documented by samples.

The analysed samples from well JA-2 and the UN-REMSA well are regarded as post glacial, but are still either of latest Hirnantian age, or at least no younger than earliest Rhuddanian if one follows Loydell's (2007) arguments for the Mauritania material. This uncertainty is indicated by a blue stripe on the graph (Fig. 5) summarising the reassessment of previously reported chitinozoan assemblages from Libya. However, an alternative interpretation, based on an environmental control of the range of the chitinozoans, cannot be definitively ruled out, even if the chitinozoans are not usually deeply affected by environmental factors. Because the *moussegoudensis* chitinozoan assemblages are so far restricted to the rather nearshore environments of the Kufra Basin (including Chad), the proliferation of *E. moussegoudaensis* may reflect an environmental control rather than a stratigraphically restricted range. If so, the absence of *E. moussegoudaensis* in Rhuddanian sections with a graptolite control (deeper

environments) would simply be a result of differences in the bathymetry of the depositional areas.

Based on the discussion above on chitinozoan biostratigraphy and palaeoecology, it appears that the studied section records an assemblage of latest Ordovician to earliest Silurian age. The acritarchs, miospores and cryptospores assemblage recorded seem to be no older than earliest Rhuddanian. However, several key post-glacial, latest Hirnantian sections, especially the Nseirat section in Mauritania and Anti-Atlas section in Morocco, where post-glacial Hirnantian chitinozoan assemblages have been documented, need to be investigated for acritarch and miospore content, for possible extension of the reported earliest Rhuddanian species to the latest Hirnantian.

Acknowledgments

We are very grateful to Faraj Said (National Oil Corporation, Tripoli, Libya), Ahmed I. Asbali (Arabian Gulf Oil Company, Benghazi, Libya), Ramadan Aburawi (Exploration Director, Libya Holdings Co.) and Bourima Belgasem (Libyan Petroleum Institute, Tripoli, Libya) for their scientific support and guidance during the project work in Libya. We also would like to thank the logistics team, provided by Bashir Grenat, for assistance in the field. The administrative and logistical support of staff at the Libyan Petroleum Institute is gratefully acknowledged. Support by the Earth Science Society of Libya is much appreciated. Special thanks go to James Stewart and Clive Johnson for their support during the drilling campaign in the Sahara Desert, to Shir Akbari for palynological sample preparation, and to John E.A. Marshall for providing chitinozoan reflectance data for some of the JA-2 core samples. The consortium of oil and gas industry subscribers is thanked for its financial support to the CASP Southern Basins of Libya

Project. Thijs R.A. Vandenbroucke and an anonoymous reviewer contributed with thoughtful comments to improve the manuscript. This paper is a contribution to the International Geoscience Programme (IGCP) Project 591 – 'The Early to Middle Paleozoic Revolution'.

Appendix A. Supplementary data

Supplementary data associated with this article can be found, in the online version, at xxx.

References

Achab, A., 1978. Les chitinozoaires de l'Ordovicien supérieur (Formations de Vauréal et d'Ellis Bay) de l'ïle d'Anticosti, Québec. Palinologia, num. extraord., 1, 1–19.

Al-Ameri, T.K., 1983. Acid resistant microfossils used in the determination of Palaeozoic palaeoenvironment in Libya. Palaeogeography, Palaeoclimatology, Palaeoecology 44, 103–116.

Al-Ameri, T.K., 1989. Chitinozoa of the Tanezzuft and Acacus Formations, Libya. Iraqi Journal of Sciences 30, 203–242.

Becip, 1974. Regional subsurface biostratigraphy of Ghadamas Basin (Internal Report). National Oil Corporation (Arabian Gulf Oil Co. Benghazi, Libya), Exploration Division Technical Library (Unpublished study).

Bourahrouh, A., 2002. Chitinozoaires et Palynomorphes de l'Ordovicien supérieur Nord-gondwanien; Impact de la Glaciation Ashgilienne. Unpublished Doctoral Thesis, Rennes University, 300 pp.

Braddy, S.J., 2001. Eurypterid palaeoecology: palaeobiological, ichnological and comparative evidence for a 'mass–moult–mate' hypothesis. Palaeogeography, Palaeoclimatology, Palaeoecology 172, 115–132.

722 Butcher, A., 2009. Early Llandovery chitinozoans from Jordan. Palaeontology 52, 593–629.
723 Butcher, A., 2012. Chitinozoans from the middle Rhuddanian (lower Llandovery, Silurian) 'hot'
724 shale in the E1-NC174 core, Murzuq Basin, SW Libya. Review of Palaeobotany and
725 Palynology, doi:10.1016/j.revpalbo.2012.11.009
726 Chen, Xu, Rong, J., Mitchell, C.E., Harper, D.A.T., Fan, J.-X., Zhan, R., Zhang, Y., Li, R.,
727 Wang, Y., 2000. Late Ordovician to earliest Silurian gaptolite and brachiopod biozonation
728 from the Yangtze region, South China, with a global correlation. Geological Magazine 137,
729 623–650.
730 Chen, Xu, Rong, J., Fan, J.-X., Zhan, R., Mitchell, C.E., Harper, D.A.T., Melchin, M.J., Peng,
731 P., Finney, S.C., Wang, X.-F., 2006. The global boundary stratotype section (GSSP) for the
732 base of the Hirnantian Stage (the uppermost of the Ordovician System). Episodes 29, 183–
733 196.
734 Da Costa, N.M., 1971. Quitinozoários silurianos do Igarapé da Rainha, Estado do Para. Estado
735 do Pará. Departamento Nacional da Produção Mineral. Divisão de Geologia e Mineralogia
736 Boletim 255, 1–101.
737 Delabroye, A., Vecoli, M., 2010. The end-Ordovician glaciation and the Hirnantian Stage: global
738 review and questions about Late Ordovician event stratigraphy. Earth-Science Reviews 98,
739 269–282.
740 De La Puente, S., 2009. Quitinozoos del Ordovicico de la Cuenca Andina central (noroeste
741 Argentino) y su aplicacion a la bioestratigrafia, paleobiologeigrafia y paleoambientes.
742 Unpublished Thesis, University of Cordoba, 246 pp.
743 Dorning, J. K., 1981. Silurian acritarch distribution in the Ludlovian shelf sea of South Wales
744 and the Welsh Borderland. In: Neale, J.W., Brasier, M.D. (Eds.), Microfossils from Recent
745 and Fossil Shelf Seas. Ellis Horwood, Chichester, 31–36.

746 Dufka, P., Fatka, O., 1993. Chitinozoans and acritarchs from the Ordovician-Silurian boundary
747 of the Prague Basin, Czech Republic. Special Papers in Palaeontology 48, 17–28.
748 Ghavidel-Syooki, M., 2008. Palynostratigraphy and palaeogeography of the Upper Ordovician
749 Gorgan schists (southeastern Caspian Sea), Eastern Alborz mountain ranges, northern Iran.
750 Comunicações Geológicas 95, 123–155.
751 Grignani, D., Lanzoni, E., Elatrash, H., 1991. Palaeozoic and Mesozoic subsurface
752 palynostratigraphy in the Al Kufrah Basin, Libya. In: Salem, M. J., Hammuda, O.S.,
753 Eliagoubi, B.A. (Eds.), The Geology of Libya, Vol. IV. Elsevier, Amsterdam, 1159–1227.
754 Hill, P.J., Molyneux, S.G., 1988. Biostratigraphy, palynofacies and provincialism of Late
755 Ordovician-Early Silurian acritarchs from northeast Libya. In: El-Arnauti, A. Owens, B.,
756 Thusu, B. (Eds.), Subsurface palynostratigraphy of northeast Libya. Garyounis University
757 Publications, Benghazi, 27–43.
758 Hill, P.J., Paris, F., Richardson, J.B., 1985. Silurian palynomorphs. In: Thusu, B., Owens, B.
759 (Eds.), Palynostratigraphy of North-East Libya. Journal of Micropalaeontology 4, 27–48.
760 International Subcomission on Silurian Stratigraphy, 2007. Final report of the Subcommission
761 on Silurian Stratigraphy restudying the Global Stratotype for the base of the Silurian: A
762 report of the restudy of the defined Global Stratotype of the base of the Silurian System.
763 Silurian Times 14, 10–13.
764 Jardiné, S., Combaz, A., Magloire, L., Peniguel, G., Vachey, G., 1974. Distribution
765 stratigraphique des Acritarches dans le Paleozoïque du Sahara Algerien. Review of
766 Palaeobotany and Palynology 18, 99–129.
767 Johnson, N.G., 1985. Early Silurian palynomorphs from the Tuscarora Formation in central
768 Pennsylvania and their paleobotanical and geological significance. Review of Palaeobotany
769 and Palynology 45, 307–360.

770 Jones, B., Kjellesvig-Waering, E.N., 1985. Upper Silurian eurypterids from the Leopold
771 Formation, Somerset Island, Arctic Canada. Journal of Paleontology 59, 411–417.
772 Keegan, J.B., Rasul, S.M., Shaheen, Y., 1990. Palynostratigraphy of the Lower Palaeozoic,
773 Cambrian to Silurian, sediment of the Hashemite Kingdom of Jordan. Review of
774 Palaeobotany and Palynology 66, 167–180.
775 Legrand, P., 2009. Faunal specificity, endemism and paleobiogeography: the post-glacial
776 (Hirnantian-early Rhuddanian) graptolite fauna of the North-African border of Gondwana: a
777 case study. Bulletin de la Société Géologique de France 180, 353–367.
778 Le Hérissé, A., Al-Tayyar, H., van der Eem, H., 1995. Stratigraphy and paleogeographic
779 significance of Silurian acritarchs from Saudi Arabia. Review of Palaeobotany and
780 Palynology 89, 49–74.
781 Le Hérissé, A., Massa, D., Paris, F., Steemans, P., 2004. Northern Gondwana palynomorphs
782 from the Ordovician-Silurian boundary beds: The example of northern Chad. Sedimentary
783 basins of Libya, Third Symposium: Geology of East Libya, Benghazi, 21-23 November
784 2004, Abstract.
785 Le Hérissé, A., Paris, F., Steemans, P., 2013. Late Ordovician–earliest Silurian palynomorphs
786 from northern Chad and correlation with contemporaneous deposits of southeastern Libya.
787 Bulletin of Geosciences, doi:10.3140/bull.geosci.1383
788 Loi, A., Ghienne, J.F., Dabard, M.P., Paris, F., Botquelen, A., Christ, N., Elaouad-Debbaj, Z.,
789 Gorini, A., Vidal, M., Videt, B., Destombes, J., 2010. The Late Ordovician glacio-eustatic
790 record from a high-latitude storm-dominated shelf succession; the Bou Ingarf section (Anti-
791 Atlas, Southern Morocco). Palaeogeography, Palaeoclimatology, Palaeoecology 296, 332–
792 358.

793 Loydell, D.K., 2007. Graptolites from the Upper Ordovician and Lower Silurian of Jordan.
794 Special Papers in Palaeontology 78, 1–66.
795 Loydell, D.K., 2012. Graptolite biostratigraphy of the E1-NC174 core, Rhuddanian (lower
796 Llandovery, Silurian), Murzuq Basin (Libya). Bulletin of Geosciences 87, 651–660.
797 Lüning, S., Craig, J., Loydell, D.K., Štorch, P., Fitches, B., 2000. Lower Silurian 'hot shales' in
798 North Africa and Arabia: regional distribution and depositional model. Earth-Science
799 Reviews 49, 121–200.
800 Lüning, S., Shahin, Y.M., Loydell, D., Al-Rabi, H.T., Masri, A., Tarawneh, B., Kolonic, S.,
801 2005. Anatomy of a world-class source rock: Distribution and depositional model of
802 Silurian organic-rich shales in Jordan and implications for hydrocarbon potential. American
803 Association of Petroleum Geologists Bulletin 89, 1397–1427.
804 Lüning, S., Loydell, D.K., Štorch, P., Shain, Y., Craig, J., 2006. Origin, sequence stratigraphy,
805 and depositional environment of an Upper Ordovician (Hirnantian) deglacial black shale,
806 Jordan—Discussion. Palaeogeography, Palaeoclimatology, Palaeoecology 230, 352–355.
807 Melchin, M.J., 2008. Restudy of some Ordovician–Silurian boundary graptolites from Anticosti
808 Island, Canada, and their biostratigraphic significance. Lethaia 41, 155–162.
809 Melchin, M.J., Williams, S.H., 2000. A restudy of the Akidograptine graptolites from Dob' Linn
810 and a proposed redefined zonation of the Silurian stratotype. In: Cockel P., Wilson, G.A.,
811 Brock, G.A., Engelbretsen, M.J., Simpson, A., Winchester-Seeto, T. (Eds.), Palaeontology
812 Down-Under 2000. Geological Society of Australia, Abstracts 61, 63.
813 Molyneux, S.G., Paris, F., 1985. Late Ordovician palynomorphs. In: Thusu, B., Owens, B.
814 (Eds.), Palynostratigraphy of North-East Libya. Journal of Micropalaeontology 4, 11–26.

Paris, F., 1988. Late Ordovician and Early Silurian chitinozoans from central and southern Cyrenaica. In: El-Arnauti, A., Owens, B., Thusu, B. (Eds.), Subsurface palynostratigraphy of Northeast Libya. Garyounis University Publications, Benghazi, Libya, 61–71.

Paris, F., 1990. The Ordovician chitinozoan biozones of the northern Gondwana Domain. Review of Palaeobotany and Palynology 66, 181–209.

Paris, F., Bourahrouh, A., Le Hérissé, A., 2000. The effects of the final stages of the Late Ordovician glaciation on marine palynomorphs (chitinozoans, acritarchs, leiospheres) in well Nl-2 (NE Algerian Sahara). Review of Palaeobotany Palynology 113, 87–104.

Paris, F., Verniers, J., Al-Hajri, S., Al-Tayyar, H., 1995. Biostratigraphy and palaeogeographic affinities of Early Silurian chitinozoans from central Saudi Arabia. Review of Palaeobotany and Palynology 89, 75–90.

Paris, F., Deynoux, M., Ghienne, J.F., 1998. Découverte de chitinozoaires à la limite Ordovicien-Silurien en Mauritanie; implications paléogéographiques. Comptes rendus de l'Academie des sciences, Series II, 326, 499–504.

Paris, F., Thusu, B., Whitham, A., Abutarruma, Y., El Dieb, M., Elkatarry, F.M., Hamhoom, A.M., Howard, J., Lüning, S., Phillips, R., 2008. Late Ordovician–Early Silurian chitinozoan biostratigraphy in Jebel Dalma, Kufra Basin, Libya. Kufra Basin Project, Unpublished CASP Report 9, 43 pp.

Paris, F., Thusu, B., Rasul, S., Meinhold, G., Strogen, D., Howard, J.P., Abutarruma, Y., Elgadry, M., Whitham, A.G., 2012. Palynological and palynofacies analysis of early Silurian shales from borehole CDEG-2a in Dor el Gussa, eastern Murzuq Basin, Libya. Review of Palaeobotany and Palynology 174, 1–26.

837 Paris, F., Verniers, J., Miller, M., Al-Hajri, S., Melvin, J., Wellman, C.H., 2013. Late
838 Ordovician–earliest Silurian chitinozoans from the Qusaiba core hole (North Central Saudi
839 Arabia) and relation to the Hirnantian glaciation. GeoArabia, Special Publication (in press)
840 Piçarra, J.M., Robardet, M., Bourahrouh, A., Paris, F., Pereira, Z., Le Menn, J., Gourvennec, R.,
841 Oliveira, T., Lardeux, H., 2002. Le passage Ordovicien-Silurien et la partie inférieure du
842 Silurien (Sud-Est du Massif Armoricain, France). Comptes Rendus Geosciences 334, 1137–
843 1183.
844 Piçarra, J.M., Robardet, M., Oliveira, J.T., Paris, F., Lardeux, H., 2009. Graptolite faunas of the
845 Llandovery "phtanites" at Les Fresnaies (Chalonnes-sur-Loire, southeastern Armorican
846 Massif): Palaeontology and biostratigraphy. Bulletin of Geosciences 84, 41–50.
847 Richardson, J.B., 1988. Late Ordovician and Early Silurian cryptospores and miospores from
848 northeast Libya. In: El-Arnauti, A., Owens, B., Thusu, B. (Eds.), Subsurface
849 palynostratigraphy of northeast Libya. Garyounis University Publications, Benghazi, Libya,
850 89–109.
851 Richardson, J.B., Ioannides, N., 1973. Silurian palynomorphs from the Tanezzuft and Acacus
852 Formations, Tripolitania, North Africa. Micropaleontology 19, 257–307.
853 Soufiane, A., Achab, A., 2000. Chitinozoan zonation of the Late Ordovician and the Early
854 Silurian of the Island of Anticosti, Québec, Canada. Review of Palaeobotany and
855 Palynology 109, 85–111.
856 Staplin, F.L., 1969. Sedimentary organic matter, organic metamorphism, and oil and gas
857 occurrences. Bulletin of Canadian Petroleum Geology 17, 47–66.
858 Štorch, P., 1996. The basal Silurian *Akidograptus ascensus-Parakidograptus acuminatus*
859 Biozone in peri-Gondwana Europe: graptolite assemblages, stratigraphical ranges and
860 palaeobiogeography. Vestnik Cekeho Geologickeho Ustavu 71, 177–188.

861 Štorch, P., Loydell, D.K., 1996. The Hirnantian graptolites *Normalograptus persculptus* and
862 '*Glyptograptus*' *bohemicus*: stratigraphical consequences of their synonymy. Palaeontology
863 39, 869–881.
864 Taugourdeau, P., 1962. Association de Chitinozoaires dans quelques sondages de la région de
865 Edjelé (Sahara). Revue de Micropaléontologie 4, 229–236.
866 Thusu, B., Syed, R., Whitham, A., Abtarruma, Y., El Dieb, M., Elkatarry, F.M., Hamhoom,
867 A.M., Howard, J., Lüning, S., Phillips, R., 2007. Sub-surface Lower Paleozoic
868 palynostratigraphy in the Kufra Basin, Libya. Kufra Basin Project, Unpublished CASP
869 Report 6, 47 pp.
870 Tricker, P.M., Marshall, J.E.A., Badman, T.D., 1992. Chitinozoan reflectance: a Lower
871 Palaeozoic thermal maturity indicator. Marine and Petroleum Geology 9, 302–307.
872 Underwood, C.J., Deynoux, M., Ghienne, J.F., 1998. High palaeolatitude (Hodh, Mauritania)
873 recovery of graptolite faunas after the Hirnantian (end Ordovician) extinction event.
874 Palaeogeography, Palaeoclimatology, Palaeoecology 142, 91–105.
875 Vandenbroucke, T.R.A., 2008. An Upper Ordovician chitinozoan biozonation in British
876 Avalonia (England and Wales). Lethaia 41, 275–294.
877 Vandenbroucke, T.R.A., Rickards, B., Verniers, J., 2005. Upper Ordovician chitinozoan
878 biostratigraphy from the Asghill (Cautley district) and Pus Gill section (Dufton dsistrict,
879 Cross Fell Inlier), Cumbria, Northern England. Geological Magazine 142, 783–807.
880 Vandenbroucke, T.R.A., Gabott, S.E., Paris, F., Aldridge, R.L., Theron, J.N., 2009. Chitinozoans
881 and the age of the Soom Shale, an Ordovician black shale Lagerstätte, South Africa. Journal
882 of Micropalaeontology 28, 53–66.

883 Verniers, J., Vandenbroucke, T.R.A., 2006. Chitinozoan biostratigraphy in the Dob's Linn
884 Ordovician-Silurian GSSP, Southern Uplands, Scotland. Geologiska Föreningens i
885 Stockholm Förhandlingar 128, 195–202.
886 Verniers, J., Nestor, V., Paris, F., Dufka, P., Sutherland, S., Van Grootel, G., 1995. A global
887 Chitinozoa biozonation for the Silurian. Geological Magazine 132, 651–666.
888 Webby, B.D., Cooper, R.A., Bergström, S.M., Paris, F., 2004. Stratigraphic Framework and time
889 slices. In: Webby, B.D., Paris, F., Droser, M., Percival, I. (Eds.), The Great Ordovician
890 Biodiversification Event. Columbia University Press, New York, 41–47.
891 Wellman, C.H., Richardson, J.B., 1993. Terrestrial plant microfossils from Silurian inliers of the
892 Midland Valley of Scotland. Palaeontology 36, 155–193.
893 Williams, S.H., Ingham, J.K., 1989. Stratotypes, 4. The Ordovician-Silurian boundary at Dob's
894 Linn, southern Scotland. In: Holland, C.H., Bassett, M.G. (Eds.), A global Standard for the
895 Silurian System. National Museum of Wales, Geological Series 9, 27–35.
896
897 **Tables**
898
899 Table 1. List of the main palynological and lithological data for the samples processed from well
900 JA-2 and the UN-REMSA well for chitinozoan analysis.
901
902 Table 2. Range and relative frequencies (counted number of species) of the acritarchs recorded
903 in the processed samples from well JA-2 and the UN-REMSA well.
904

905 Table 3. Range and relative frequencies (counted number of species) of the sporomorphs and
906 *Tortubus portuberans* recorded in the processed samples from well JA-2 and the UN-REMSA
907 well.
908
909 Table 4. Kerogen analysis data (grain count of all sizes undertaken under transmitted light) on
910 samples from well JA-2 and on cutting samples (SJS0001) from the UN-REMSA well. Numbers
911 are in percentages.
912
913 Table 5. Chitinozoan reflectance (R_{ch}) values in % of core samples from well JA-2 (provided by
914 John E. A. Marshall, University of Southampton). The measured reflectance values (average)
915 have been corrected against a standard which was measured at the start and end of every sample
916 series. For every sample the corrected value is close to the average value, showing that there has
917 been not much instrumental drift during reflectance measurements. The vitrinite reflectance (R_v)
918 values in % were calculated using the equation in Tricker et al. (1992).
919
920 **FIGURE CAPTIONS**
921
922 Fig. 1. Map of Libya showing surface outcrops with Paleozoic rocks (dark grey colour) and the
923 location of Jebel Asba at the eastern margin of the Kufra Basin (after Paris et al., 2012). The drill
924 site localities of well CDEG-2a in central Dor el Gussa (Paris et al., 2012) and well JA-2 in
925 southern Jebel Asba (this study) are indicated. The UN-REMSA well was found some 530 m
926 towards the NNE from JA-2 (not shown in the map).
927

928 Fig. 2. Lithological log of the core from well JA-2 together with biostratigraphic age,
929 chitinozoan abundance and kerogen analysis data (see also Table 4). See text for explanation
930
931 Fig. 3. Selected palynomorph species with stratigraphic ranges and regional occurrences in
932 North Africa, the Middle East and USA (Becip, 1974; Jardiné et al., 1974; Johnson, 1985;
933 Molyneux and Paris, 1985; Hill and Molyneux, 1988; Keegan et al., 1990; Le Hérissé et al.,
934 1995; Paris et al., 2012) and comparison with the present study.
935
936 Fig. 4. Range, relative frequencies and abundances of the chitinozoans recorded in the processed
937 samples from well JA-2.
938
939 Fig. 5. Correlation table for some Gondwana chitinozoan-bearing strata around the Ordovician-
940 Silurian boundary and their relative stratigraphical position with regard to the range of the main
941 diagnostic chitinozoan species, and to the standard graptolite biozones. 1: F. Paris, unpublished
942 data, 2: Grignani et al., 1991; 3: Paris et al., 2008; 4: Molyneux and Paris, 1985; 5: Paris, 1988;
943 6: Paris et al., 2012; 7: Le Hérissé et al., 2013; 8: Butcher, 2009; 9: Paris et al., 1998; 10:
944 Vandenbroucke et al., 2009; 11, Bourahrouh, 2002; 12: Piçarra et al., 2002; 13: Dufka and Fatka,
945 1993. Red line: exclusive Late Ordovician species; blue line: exclusive early Silurian taxa; black
946 line: taxa ranging possibly through the Ordovician–Silurian boundary. The blue stripe
947 corresponds to a brief but poorly constrained time slice of uppermost Hirnantian or lowermost
948 Rhuddanian age (i.e. “interregnum” between the top of the *persculptus* and the base of the
949 *ascensu*s graptolite biozones; see discussion in Legrand, 2009).
950
951 **PLATES**

Plate I. Scale bar = 10 μm.

1: *Rugosphaera tuscarorensis* Strother & Traverse, 1979. Slide no. 5758-3. Core sample at 57.58 m depth. England finder location: S34-1.

2: *Lophozonotriletes* sp. Slide no. 5758-3. Core sample at 57.58 m depth. England finder location: S34-4.

3: *Tortotubus protuberans* Johnson, 1985. Slide no. 5758. Core sample at 57.58 m depth. England finder location: L28.

4: *Ambitisporites dilutus* (Hoffmeister) Richardson & Lister, 1969. Slide no. 5553. Core sample at 55.53 m depth. England finder location: T10.

5: *Dyadosphaera murusdensa* Strother & Traverse, 1979. Slide no. 5758. Core sample at 57.58 m depth. England finder location: V37.

6: *Ambitisporites dilutus* (Hoffmeister) Richardson & Lister, 1969. Slide no. 6759. Core sample at 67.59 m depth. England finder location: H45-2. Note: The slide number corresponds to the core sample depth in cm.

7: *Ambitisporites dilutus* (Hoffmeister) Richardson & Lister, 1969. Slide no. 6782-5. Core sample at 67.82 m depth. England finder location: L31-2.

8: *Tetrahedraletes medinensis* Strother & Traverse, 1979, emend. Wellman and Richardson, 1993. Slide no. 6782-5. Core sample at 67.82 m depth. England finder location: K31-2.

Plate II. Scale bar = 10 μm.

1: *Rugosphaera tuscarorensis* Strother & Traverse, 1979. Slide no. 5758. Core sample at 57.58 m depth. England finder location: J37-1.

2: *Dyadosphaera murusdensa* Strother & Traverse, 1979. Slide no. 5758. Core sample at 57.58 m depth. England finder location: f41-2.

3: *Tetrahedraletes medinensis* Strother & Traverse, 1979, emend. Wellman & Richardson, 1993. Slide no. 5758. Core sample at 57.58 m depth. England finder location: J29-2.

4: *Veryhachium lairdii* group (Deflandre) Deunff, 1954 ex Loeblich, 1970. Slide no. 6782-5. Core sample at 67.82 m depth. England finder location: W28.

5: *Archaeozonotriletes chulus var. chulus* (Cramer) Richardson & Lister, 1969. Slide no. 6759. Core sample at 67.59 m depth. England finder location: J29-3.

6: *Dyadosphaera murusdensa* Strother & Traverse, 1979. Slide no. 6782. Core sample at 67.82 m depth. England finder location: F21-1.

7: *Tasmanites* sp. Slide no. 4818. Core sample at 48.18 m depth. England finder location: J41.

8: *Veryhachium lairdii* group (Deflandre) Deunff, 1954 ex Loeblich, 1970. Slide no. 6782-5. Core sample at 67.82 m depth. England finder location: X21-1.

Plate III. Scale bar = 10 μm.

1: *Leiosphaeridia* sp. Slide no. 5758-1. Core sample at 57.58 m depth. England finder location: R44-3.

2: *Rugosphaera* sp. Slide no. 5758-2. Core sample at 57.58 m depth. England finder location: T22.

3: *Leiosphaeridia acerscabrella* Johnson, 1985. Slide no. 6782-5. Core sample at 67.82 m depth. England finder location: T34-2.

4: *Leiosphaerida* sp. (in clusters). Slide no. 6782-5. Core sample at 67.82 m depth. England finder location: K32

5: *Filisphaeridium* sp. Slide no. 6782-5. Core sample at 67.82 m depth. England finder location: H32-4.

6: *Solisphaeridium* sp. Slide no. 6759. Core sample at 67.59 m depth. England finder location: W23-4.

7: *Diexallophasis denticulata* (Stockmans & Williere) Loeblich, 1970. Slide no. 6782. Core sample at 67.82 m depth. England finder location: V31-2.

8: *Diexallophasis denticulata* (Stockmans & Williere) Loeblich, 1970. Slide no. 6782-5. Core sample at 67.82 m depth. England finder location: F18-2.

Plate IV. Scale bar = 10 μm.

1: *Eupoikilofusa striatifera* Cramer, 1970. Slide no. 4818-4. Core sample at 48.18 m depth. England finder location: M19.

2: *Eupoikilofusa striatifera* Cramer, 1970. Slide no. 5758-3. Core sample at 57.58 m depth. England finder location: W22.

3: *Leiofusa estrecha* Cramer, 1964. Slide no. 6782-5. Core sample at 67.82 m depth. England finder location: H31-4.

4: *Moyeria cabottii* (Cramer) Miller & Eames, 1982. Slide no. 6782-5. Core sample at 67.82 m depth. England finder location: K32-2.

5: *Veryhachium trispinosum* (Eisenack) Stockmans & Williere, 1962. Slide no. 4818-4. Core sample at 48.18 m depth. England finder location: V24

6: *Geron* cf. *gracilis* Cramer, 1969. Note that the tail like feature characteristic in genus *Geron* is visible in phase contrast only. Slide no. 5758-1. Core sample at 57.58 m depth. England finder location: D3-2.

7: *Veryhachium trispinosum* (Eisenack) Stockmans & Williere, 1962. Slide no. 5758-1. Core sample at 57.58 m depth. England finder location: W19-2.

8: *Veryhachium europaeum* Stockmans & Williere, 1960, 1954 ex Loeblich, 1970. Slide no. 5758-2. Core sample at 57.58 m depth. England finder location: Q27-3.

Plate V. Scale bar = 10 μm.

1: *Micrhystridium* sp. (8 spined form). Slide no. 6721. Core sample at 67.21 m depth. England finder location: U23.

2. *Veryhachium trispinosum* (Eisenack) Stockmans & Williere, 1962. Slide no. 6721. Core sample at 67.21 m depth. England finder location: M13.

3: *Veryhachium trispinosum* (Eisenack) Stockmans & Williere, 1962. Slide no. 6782-5. Core sample at 67.82 m depth. England finder location: K26-2.

4: *Veryhachium europaeum* Stockmans & Williere, 1960. Slide no. 6782-5. Core sample at 67.82 m depth. England finder location: G28-1.

5: *Veryhachium trispinosum* (Eisenack) Stockmans & Williere, 1962. Slide no. 6782-5. Sample at 67.82 m depth. England finder location: G33-3.

6: *Veryhachium* sp. (4 spined). Slide no. 6782-5. Core sample at 67.82 m depth. England finder location: J24-4.

7: *Micrhystridium* sp. (8 spined). Slide no. 6782-5. Core sample at 67.82 m depth. England finder location: K34-1.

8: *Veryhachium lairdii* (Deflandre) Deunff, 1954 ex Loeblich, 1970. Slide no. 6782-5. Core sample at 67.82 m depth. England finder location: Q21.

Plate VI. Scale bar = 100 μm, except for 1b, 2b, 3b, 4b, 6b, 7b and 9b (10 μm).

1a−b, 2a−b: ?*Spinachitina verniersi* Vandenbroucke, in Vandenbroucke et al., 2009. Core sample at 55.53 m depth; IGR 72962. 1a (O49/3): conical specimen with gently tapering flanks and granules/spines concentrated on the margin. 1b: close-up of the granules/spines (less than 2 microns length, but possibly eroded) concentrated on the margin. Some granules seem also scattered on the chamber. 2a (N44/4): flattened specimen (vesicle of 150 μm length) with a tilted bottom. 2b: close-up of the spines (up to 2 μm length) erected on the margin (not exactly arranged in a single row).

3a−b: *Spinachitina verniersi* Vandenbroucke, in Vandenbroucke et al., 2009. Core sample at 55.53 m depth; IGR 72962 (L47/4). 3a: conical vesicle showing the diagnostic crown of densely distributed spines/granules on the margin. 3b: detail of the spines/granules (up to 3 μm length) forming a crown around the carina.

4a−b, 8a−b: *Euconochitina moussegoudaensis* Paris, in Le Hérissé et al., 2013. Core sample at 67.82 m depth; IGR 72987. 4a (O47/2): conical specimen with gently tapering flanks and a slightly flaring collarette. 4b: close-up of the smooth wall surface. 8a (O47/3): specimen (vesicle of 146 μm length) with a partly tilted bottom. 8b: close-up of the margin devoid of spines or granules.

5: *Plectochitina* cf. *longispina* (Achab, 1978). Core sample at 67.82 m depth; 72987 (L38/3).

6a−b: ?*Spinachitina verniersi* Vandenbroucke, in Vandenbroucke et al., 2009. Core sample at 60.23 m depth; IGR 729864 (O47). 6a (O47/2): conical specimen with gently tapering flanks. 6b: close-up of the margin showing possible granules in row.

7a−b: ?*Spinachitina verniersi* Vandenbroucke, in Vandenbroucke et al., 2009. Core sample at 67.82 m depth; IGR 72987 (L43/1). 7a: long conical specimen with a gently flaring collarette and spines concentrated on the margin. 7b: close-up showing the spines (up to 3 μm length) concentrated on the margin. Some granules (less than 1 μm length) seem also scattered on the lower part of the chamber.

9: *Plectochitina* sp. Core sample at 60.23 m depth; IGR 72964 (N45/1). Note the long processes branched at their distal part (most of them are broken). The neck is likely damaged.

10: *Plectochitina* cf. *longispina* (Achab, 1978). Core sample at 67.82 m depth; IGR 72987 (M46). Specimen with a long neck ended by a flaring collarette. The processes branch at their about 2/3 of their length.

Plate VII. Scale bar = 100 μm, except for 1b, 1c, 2b, 3b, 4b, 9b and 9c (10 μm).

1a−c, 3a−b, 4a−b, 6, 8, 9a−c: *Spinachitina oulebsiri* Paris et al., 2000. Core sample at 67.59 m depth; IGR 72981. 1a (M44/1): typical specimen with a well-developed crown of spines (about 20 spines) erected around its margin. 1b: close-up of the spines (up to 8 μm length) showing their slender conical shape and their widened hollow base. 1c: detail of the wall surface, which seems rough at high magnification (possibly covered by a bacterial mat). 3a (Q47/1): fairly long specimen (vesicle of

170 µm length) with a well-developed crown of spines (about 24 spines) around its margin and a conspicuous supra-margin constriction. 3b: close-up of the spines (up to 8 µm length) erected on the margin showing their slender conical shape and their widened hollow base. 4a (L48): long specimen (vesicle of 190 µm length) with a well-developed crown of spines (about 20 spines) around its margin. The supra-margin constriction is weak. 4b: close-up of the slender conical spines (up to 11 µm length); note the bi-rooted base (possibly resulting of the collapse of the wall of the hollow base). 6 (L48/4): short conical vesicle (vesicle of 130 µm length). 8 (O49): very short vesicle (close to 100 µm), note the serrated aperture. 9a (Q49/4): unusual long vesicle (length close to 300 µm) with a conspicuous supra-margin constriction and a fenestrate aperture. 9b: close-up of the crown of densely distributed spines (about 30). 9c: close-up of the fenestrate aperture.

2a–b: *Spinachitina verniersi* Vandenbroucke, in Vandenbroucke et al., 2009. Core sample at 67.59 m depth; IGR 72981 (Q47). 2a: conical vesicle showing the diagnostic crown of densely distributed granules on the margin. 2b: detail of the granules arranged in a crown on the carina.

5: *Euconochitina moussegoudaensis* Paris, in Le Hérissé et al., 2013. Core sample at 67.59 m depth; IGR 72981 (P47/3).

7. ?*Spinachitina verniersi* Vandenbroucke, in Vandenbroucke et al., 2009. Core sample at 67.59 m depth; IGR 72981 (N49/3). Vesicle with granules concentrated on the margin. However, they are not clearly arranged in crown.

Plate VIII. Chitinozoans and one scolecodont from cuttings (no depth provided) from the UN-REMSA well, Kufra Basin, Libya; IGR 72995. Scale bar = 100 µm, except for 3b, 5b, 6b, 8, 9b, 10b (10 µm) and 6c (1 µm).

1: *Cyathochitina caputoi* Da Costa, 1971. (Q44); note the thick carina and the longitudinal ridges at the junction of the chamber and of the neck.

2: Scolecodont partly "coated" with amorphous organic matter (R45/4).

3a–b, 4, 5a–b: *Euconochitina moussegoudaensis* Paris, in Le Hérissé et al., 2013. 3a (S46): slightly conical specimen with a well-developed cylindrical neck. 3b: close-up of the margin devoid of spines. The granules (about 1 µm) represent likely organic particles stuck on the margin. 4 (U48): gently tapering conical vesicle without any ornamentation on its margin. 5a (S48): slender conical specimen (vesicle of 161 µm length). 5b: close-up of the margin showing minute granules (less than one µm) concentrated around the base.

6a–c, 9a–b, 10a–b: *Spinachitina verniersi* Vandenbroucke, in Vandenbroucke et al., 2009. 6a (P45/2): conical vesicle showing the diagnostic crown of densely distributed granules on the margin. 6b: detail of the crown of granules. 6c: close-up of the granules more or les in row on the margin. 9a (O48/1): long conical vesicle (190 µm length). 9b: detail of the crown of eroded granules. 10a (P49/3): conical vesicle (161 µm length) with densely distributed granules more or less forming a crown on the margin. 10b: detail of the crown of granules on the margin; additional minute granules are randomly scattered on the lower part of the chamber.

7–8: Ancyrochitininae indet. 7 (N44): damaged vesicle (broken processes) coated with amorphous organic matter. 8 (L47/4): antiapertural view of a specimen with broken processes.

Plate IX. Scale bar = 100 μm, except for 4, 7, 8 (10 μm) and 3, 5 and 10 (1 μm).

1, 6−8: *Tortotubus protuberans* Johnson, 1985. 1: Core sample at 60.23 m depth; IGR 72964 (O43); long branched structure. 6: Core sample at 67.59 m depth; IGR 72981 (P45/3); fragment of branched structure. 7: Close up of fig. 6 showing bulb-like "vesicles" at the junction between the four branches. 8: Close up showing detail of the bulb-like "vesicles" protruding on the surface of the longest branch of fig. 6.

2−5: Amorphous organic matter (biofilm) after oxidation with HNO_3. Core sample at 67.40 m depth; IGR 72979. 2: Large fragment of organic "sheet". 3: Tilted view of the "sheet" showing the spongy structure of the section. 4: Fragment of "sheet"; see the straight border of a few μm thick. 5: Casts of framboids of pyrite after dissolution with HNO_3.

9: Chitinozoan specimen (Ancyrochitininae) adhesively associated with amorphous organic matter (biofilm). Core sample at 67.82 m depth; IGR 72987 (K43/2).

10: "Sheets" of amorphous organic matter (biofilm). Core sample at 67.82 m depth, IGR 72987. Detail of the cast of framboids of pyrite when dissolved with HNO_3.

Plate X. Scale bar = 100 μm, except for 13 and 21b (50 μm).

1: *Euconochitina moussegoudaensis* Paris, in Le Hérissé et al., 2013. Core sample at 46.60 m depth; IGR 72954 (L48). Short thickset specimen.

2: *Euconochitina* cf. *moussegoudaensis* Paris, in Le Hérissé et al., 2013. Core sample at 46.60 m depth; IGR 72954 (H40). Elongate and slender specimen showing a supra-margin constriction.

3: *Euconochitina* cf. *moussegoudaensis* Paris, in Le Hérissé et al., 2013. Core sample at 48.18 m depth; IGR 72957 (H50/1). Very long specimen.

4: ?*Euconochitina moussegoudaensis* Paris, in Le Hérissé et al., 2013. Core sample at 50.73 m depth; IGR 72962 (M46). Teratological specimen with a sleeve gaining the lower vesicle and extending around the succeeding one .

5: *Euconochitina moussegoudaensis* Paris, in Le Hérissé et al., 2013. Core sample at 50.73 m depth; IGR 72958 (R40/3).

6: *Euconochitina moussegoudaensis* Paris, in Le Hérissé et al., 2013. Core sample at 55.07 m depth; IGR 72959 (S36).

7: *Euconochitina moussegoudaensis* Paris, in Le Hérissé et al., 2013. Core sample at 60.23 m depth; IGR 72965 (M39/1). Short specimen.

8, 10: *Euconochitina moussegoudaensis* Paris, in Le Hérissé et al., 2013. Core sample at 64.02 m depth; IGR 72967. 8 (G32/4). 10: short specimen (G41/2).

9: *Euconochitina* cf. *moussegoudaensis* Paris, in Le Hérissé et al., 2013. Core sample at 64.02 m depth; IGR 72967 (G38/4). Elongate and slender specimen with a supra-margin constriction.

11: *Euconochitina* cf. *moussegoudaensis* Paris, in Le Hérissé et al., 2013. Core sample at 65.74 m depth; IGR 72968 (O42). Elongate and slender specimen with a supra-margin constriction.

12: *Euconochitina moussegoudaensis* Paris, in Le Hérissé et al., 2013. Core sample at 65.74 m depth; IGR 72968 (P43/3). Short and thickset specimen.

13: *Calpichitina* sp. Core sample at 66.85 m depth; IGR 72970 (J50/2).

14−16: *Euconochitina moussegoudaensis* Paris, in Le Hérissé et al., 2013. Core sample at 66.85 m depth. 14: (N39); 15: (L45); 16 (T34/4).

17: Ancyrochitinidae indet. Core sample at 67.05 m depth (H44).

18: *Euconochitina moussegoudaensis* Paris, in Le Hérissé et al., 2013. Core sample at 67.05 m depth. Short and thickset specimen (Q41/1).

19−20: *Euconochitina* cf. *moussegoudaensis* Paris, in Le Hérissé et al., 2013. Core sample at 67.05 m depth; IGR 72974. Elongate and slender specimens with a weakly expressed supra-margin constriction. 19 (Q42); 20 (K49/1).

21a−b: *Spinachitina* cf. *S. oulebsiri* Paris et al., 2000. Core sample at 62.34 m depth; IGR 72966 (F.35/4); 21b: close-up showing the spines on the margin.

Plate XI. Scale bar = 100 μm.

1: *Spinachitina oulebsiri* Paris et al., 2000. Core sample at 67.21 m depth; IGR 72975 (F37/4).

2: *Spinachitina* cf. *verniersi* Vandenbroucke, in Vandenbroucke et al., 2009. Core sample at 67.21 m depth; IGR 72975 (M45). Specimen showing a conspicuous supra-margin constriction.

3: *Euconochitina* cf. *moussegoudaensis* Paris, in Le Hérissé et al., 2013. Core sample at 67.21 m depth; IGR 72975 (N47/2).

4: *Spinachitina* cf. *verniersi* Vandenbroucke, in Vandenbroucke et al., 2009. Core sample at 67.40 m depth; IGR 72976 (M38/2). Short specimen.

5: *Euconochitina* cf. *moussegoudaensis* Paris, in Le Hérissé et al., 2013. Core sample at 67.40 m depth; IGR 72976 (035).

6: *Spinachitina oulebsiri* Paris et al., 2000. Core sample at 67.59 m depth;72982 (L52). Abnormally short specimen.

7−10: *Spinachitina oulebsiri* Paris et al., 2000. Core sample at 67.59 m depth; 72982. 7: short specimen (M45). 8: (O36). 9: slender specimen (V49). 10: (O47)

11: *Euconochitina* cf. *moussegoudaensis* Paris, in Le Hérissé et al., 2013. Core sample at 67.82 m depth; 72982 (K44/2). Elongate and slender specimen with a supra-margin constriction and a uncommon well-developed neck.

12: *Euconochitina* sp. aff. *vitrea* (Taugourdeau, 1962). Core sample at 67.82 m depth; IGR 72985 (K40/1).

13−15, 17: *Plectochitina* cf. *longispina* (Achab, 1978). Core sample at 67.82 m depth; IGR 72985. 13: well-developed neck and broken processes (L48/4). 14: long branched processes (R34/3). 15: note the spongy processes (K46/1). 17: specimen with well-branched processes stuck on a biofilm (S37/4).

16: *Euconochitina moussegoudaensis* Paris, in Le Hérissé et al., 2013. Core sample at 67.97 m depth; IGR 72988 (O44/3).

18−20: *Euconochitina moussegoudaensis* Paris, in Le Hérissé et al., 2013. Cuttings from UN-REMSA well; IGR 72955 18: (L43/2); 19: (O37/3); 20: (P39/4).

21: *Cyathochitina caputoi* Da Costa, 1971. Cuttings from UN-REMSA well; IGR 72995 (K38).

Plate XII. Scale bar = 100 μm, except for 7, 8, 10−13 and 19 (50 μm).

1−2, 17: Scolecodont indet. 1: Core sample at 46.60 m depth; IGR 72954 (O43/3). 2: Core sample at 48.18 m depth; IGR 72957 (U42). 17: Core sample at 67.21 m depth; IGR 729575 (M39/3).

3−6: Eurypterid remains. Core sample at 50.73 m depth; IGR 72958. 3: fragment of cuticle (M41/1). 4: fragment of cuticle of a ventral segment (P44/1). 5: “sensorial hair” (P34/1). 6: claw? (M41/1).

7: Ornamented palynomorph recalling *Tasmanites tzadiensis* La Hérissé, in Le Hérissé et al., 2013. Core sample at 50.73 m depth; IGR 72958 (S34).

8, 11−13: *Tasmanites tzadiensis* Le Hérissé, in Le Hérissé et al., 2013. 7: Core sample at 50.73 m depth (S34). 8: Core sample at 50.73 m depth (Q42/3). 11: Core sample at 60.23 m depth (J28/1). 12: Core sample at 62.34 m depth (M39). 13: Core sample at 66.85 m depth (L47/1).

9, 14, 18: *Tortotubus protuberans* Johnson, 1985. 9: Core sample at 57.58 m depth; IGR 72963 (M51); branched structure. 14: Core sample at 66.85 m depth; IGR 72970 (U48/1); fragment. 18: Core sample at 67.21 m depth; IGR 72975 (S43); branched element.

10: Connected palynomorphs. Core sample at 57.58 m depth; IGR 72963 (N47/4).

15−16: “Sheets or blades” of amorphous organic matter (biofilm). Core sample at 66.85 m depth. 15: framboids of pyrite removed (circular depressions) after oxidation with HNO_3. IGR 72973 (N39/2). 16: biofilm without oxidation by HNO_3 showing black microspheres representing framboids of pyrite; IGR 72972 (P45/1).

19: ?Colony of cyanobacteria. Core sample at 67.97 m depth; IGR 72988 (R50/2).

Figure 1

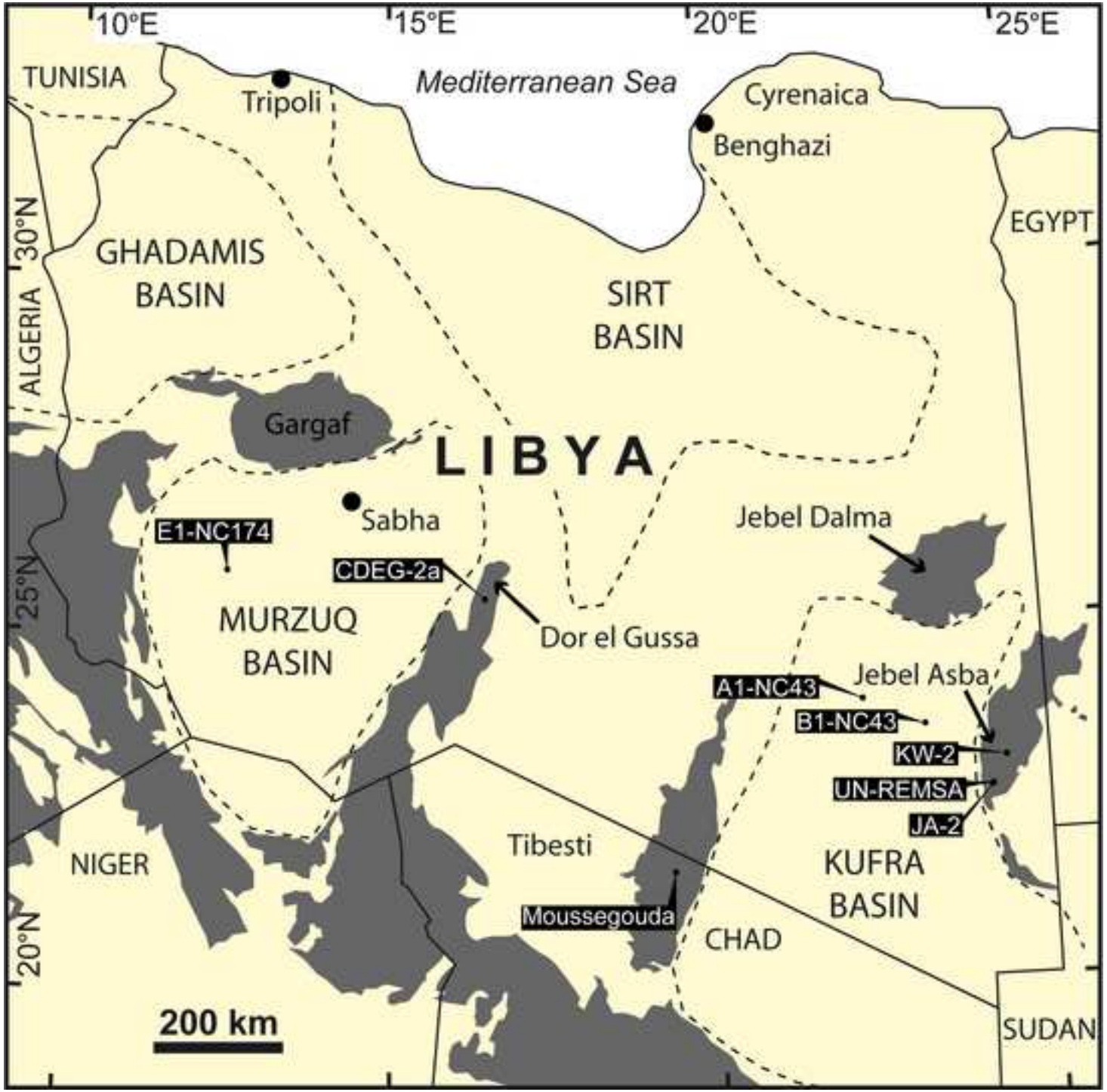
10°E
15°E
20°E
25°E
30°N
25°N
20°N
TUNISIA
Tripoli
Mediterranean Sea
Cyrenaica
Benghazi
EGYPT
ALGERIA
GHADAMIS BASIN
SIRT BASIN
Gargaf
LIBYA
Sabha
E1-NC174
CDEG-2a
Dor el Gussa
Jebel Dalma
MURZUQ BASIN
A1-NC43
Jebel Asba
B1-NC43
KW-2
UN-REMSA
JA-2
NIGER
Tibesti
KUFRA BASIN
Moussegouda
CHAD
SUDAN
200 km

Figure 2

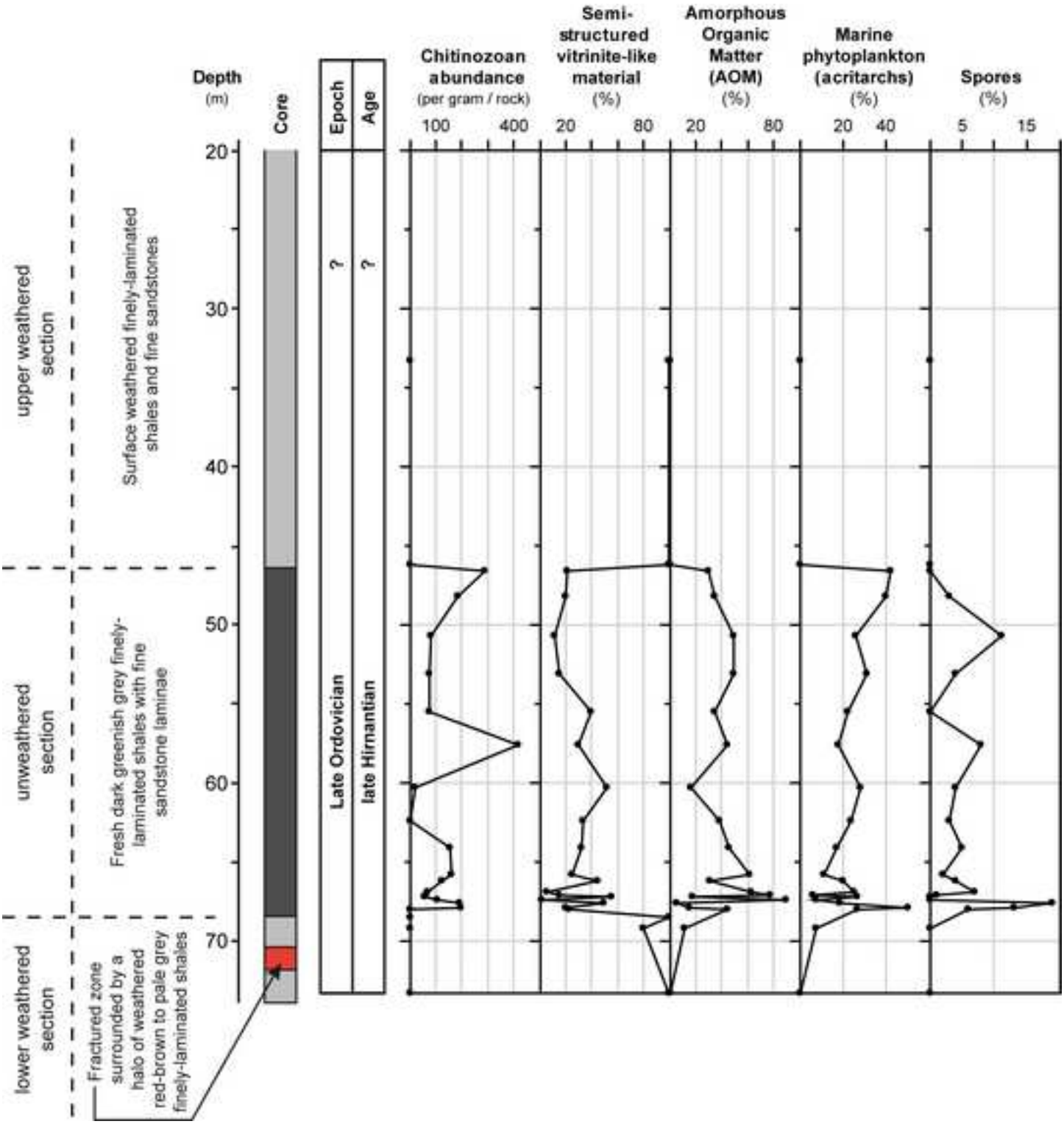
Depth
(m)
Core
Epoch
Age
Late Ordovician
late Hirnantian
?
?
Chitinozoan abundance
(per gram / rock)
100
400
Semi-structured vitrinite-like material
(%)
20
80
Amorphous Organic Matter (AOM)
(%)
20
80
Marine phytoplankton (acritarchs)
(%)
20
40
Spores
(%)
5
15
20
30
40
50
60
70
upper weathered section
unweathered section
lower weathered section
Surface weathered finely-laminated shales and fine sandstones
Fresh dark greenish grey finely-laminated shales with fine sandstone laminae
Fractured zone surrounded by a halo of weathered red-brown to pale grey finely-laminated shales

Figure 3


Ordovician
Silurian
Caradocian
Ashgillian
Llandoverian
AGE
SELECTED SPECIES
1. Eupoikilofusa striatifera
2. Veryhachium trispinosum
3. Diexallophasis denticulata
4. Leiosphaeridia acerscrabrella
5. Moyeria cabottii
6. Veryhachium europaem
7. Leiofusa estrecha
8. Tunisphaeridium sp.
9. Geron cf. gracilis
10. Filisphaeridium sp.
11. Buedingiispaeridium sp.
12. Tetrahedraletes medienensis
13. Ambitisporites dilutus
14. Archaeozonotriletes chulus var. chulus
15. Tortotubus protuberans
16. Rugosphaera tuscarorensis
17. Dyadosphaera murusdensa
No previous record from Silurian
KUFRA
LIBYA
1, 2, 3, 6, 7, 11, 12, 17
Paris et al. (2012)
MURZUQ
1, 2, 3, 7, 9, 12, 14, 17
Becip (1974) and unpublished data
GHADAMIS
1, 2, 3, 8, 11, 12, 13, 17
Molyneux and Paris (1985); Hill and Molyneux (1988)
NE LIBYA
Zone LL1-LL2
1, 2, 3, 7
Jardiné et al. (1974)
ALGERIA
Zone G1-G2
No previous record from Silurian
MOROCCO
1, 3, 5, 8, 9, 10, 11
Le Hérissé et al. (1995)
SAUDI ARABIA
Zone 2-3
9, 13, 14, 17
Keegan et al. (1990)
JORDAN
Zone JS-3
4, 12, 13, 15, 16
Johnson (1985)
PENNSYL-VANIA
USA

Figure 4

JA-2 (depth in m)	*Euc. moussegoudaensis*	*E. cf. moussegoudaensis*	*Euconochitina* sp.	*Plectochitina sp.*	*Spinachitina sp.*	*Eucono. sp. aff. vitrea*	*Spinachitina verniersi*	*Calpichitina sp.*	Ancyrochitininae indet.	*Spinachitina oulebsiri*	*Plecto cf. longispina*	*Belonechitina* sp.	Conochitinidae indet.	Chitinozoan abundance per gam / rock
33.33	100													<1
46.20	100													<1
46.60	98	<1	<1											292
48.18	98	<1	<1	<1										189
50.73	98		2											82
53.07	99		<1											74
55.53	99						<1							75
57.58	98	<1	<1											415
60.23	98						?				<1			23
62.34	96				3					cf.				5
64.02	95	1	4											128
65.74	96	2				<1	<1							160
66.21	99		<1											157
66.85	98		<1					<1						72
67.05	96	2							<1	cf.				61
67.21	96	<1					cf.		1	2				59
67.40	96						2			2				109
67.59	44	<1					20		<1	35				190
67.82	26	<1		<1		<1	?				70	<1		197
67.97	85			15										3
68.42														/
69.12	100													<1
73.21													100	<1

Figure 5

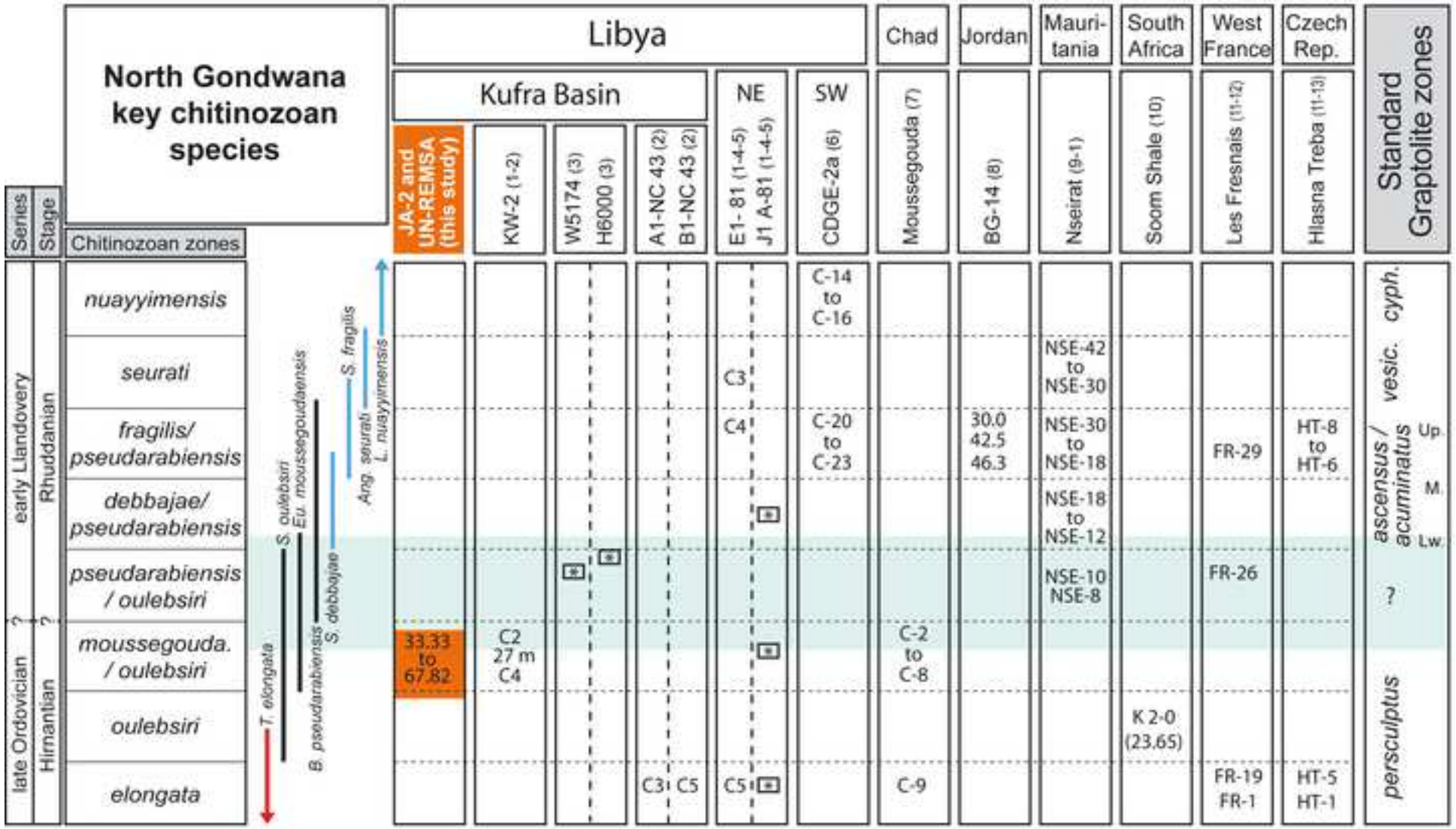
North Gondwana key chitinozoan species
Series
Stage
Chitinozoan zones
late Ordovician
early Llandovery
Hirnantian
Rhuddanian
nuayyimensis
seurati
fragilis/ pseudarabiensis
debbajae/ pseudarabiensis
pseudarabiensis / oulebsiri
moussegouda. / oulebsiri
oulebsiri
elongata
T. elongata
S. oulebsiri
Eu. moussegoudaensis
B. pseudarabiensis
S. debbajae
Arg. seurati
S. fragilis
L. nuayyimensis
Libya
Kufra Basin
JA-2 and UN-REMSA (this study)
KW-2 (1-2)
W5174 (3)
H6000 (3)
A1-NC 43 (2)
B1-NC 43 (2)
NE
E1- 81 (1-4-5)
J1 A-81 (1-4-5)
SW
CDGE-2a (6)
Chad
Moussegouda (7)
Jordan
BG-14 (8)
Mauri-tania
Nseirat (9-1)
South Africa
Soom Shale (10)
West France
Les Fresnais (11-12)
Czech Rep.
Hlasna Treba (11-13)
Standard Graptolite zones
C3
C4
C5
C-14 to C-16
C-20 to C-23
30.0
42.5
46.3
NSE-42 to NSE-30
NSE-30 to NSE-18
NSE-18 to NSE-12
NSE-10
NSE-8
FR-29
FR-26
FR-19
FR-1
HT-8 to HT-6
HT-5
HT-1
33.33 to 67.82
C2
27 m
C4
C-2 to C-8
C-9
K 2-0
(23.65)
cyph.
vesic.
ascensus / acuminatus
persculptus
Up.
M.
Lw.

Table 1

Table 1.

Sample depth (m)	Available sample (g)	Processed sample (g)	SEM observation	Chitinozoan abundance per gram / rock	Sorted %	Biofilm	Scolecodonts	Eurypterids	*Tasmanites*	Lithology	Traces of weathering
JA-2											
33.33	10.4	4.0		<1	100	X				beige silty shale	XX
46.20	10.9	5.6		<1	100	X	X			beige silty shale	X
46.60	10.2	5.0	YES	292	10	X	X		X	grey silty shale	
48.18	11.3	5.6		189	62		X			grey silty shale	
50.73	9.3	4.3		82	90		X	X	X	grey silty shale	
53.07	6.7	4.0		74	50	XX				grey silty shale	
55.53	14.3	6.0	YES	75	100					grey shale	
57.58	11.6	5.1		415	10					grey siltst., micas	
60.23	7.1	5.1	YES	23	100			X	X	grey siltst., micas	
62.34	8.5	5.1		5	100			X	X	grey siltst., micas	
64.02	11.3	7.0		154	10	X		X		grey siltstone	
65.74	7.7	5.0		160	10	X				grey shale	
66.21	14.5	7.0		128	10	XX				grey shale	
66.85	10.0	5.1		72	20	XX			X	grey shale	
67.05	5.0	3.5		61	80	XX				greenish shale	
67.21	5.6	3.7		59	90	XX	X			greenish shale	
67.40	4.6	3.3	YES	109	80	XX				greenish shale	
67.59	8.0	5.0	YES	190	10	X				grey shale	
67.82	4.4	3.2	YES	197	50	XX				fine beige sand.	
67.97	3.8	2.4		3	100				X	fine beige sand.	X
68.42	5.2	3.2		/	100					fine beige sand.	X
69.12	8.6	5.2		<1	100	X				whitish	XX
73.21	11.3	5.0		<1	100	X				grey shale	
UN-REMSA											
SJS0001		4.0	YES	125	10	X	X			dark silty shale	

Explanation: X (present), XX (abundant)

Table 2

Table 2.

Sample depth (m)	*Leiosphaeridia* spp.	*Solisphaeridium* spp.	*Eupoikilofusa striatifera*	*Tasmanites* spp.	*Veryhachium trispinosum*	*Veryhachium trispinosum (large)*	*Leiosphaeridia* spp. (clusters of small)	*Veryhachium* sp. (4 spined)	*Dictyotidium* spp.	*Leiosphaeridia* spp. clusters	*Diexallophasis denticulata*	*Geron* cf. *gracilis*	*Leiofusa* sp.	*Multiplicisphaeridium* spp.	*Veryhachium europaeum*	*Veryhachium lairdii*	*Filisphaeridium sp.*	*Micrhystridium* sp. (8 spined)	*Diexallophasis* spp.	*Leiosphaeridia* spp. (small)	*Veryhachium* sp. cluster	*Cymatiosphaera* spp.	*Tunisphaeridium* spp.	*Goniosphaeridium* spp.	*Leiosphaera small*	*Buedingiisphaeridium*sp.	*Leiofusa estrecha*	*Leiosphaeridia acerscarbrella*	*Moyeria cabottii*	*Veryhachium trispinosum (globular form)*
JA-2																														
33.33																														
46.20																														
46.60	C	R																												
48.18	C		R	R	R	R																								
50.73	C		C				R	R																						
53.07	C		R		R		R		C	R																				
55.53	A		R	R						R																				
57.58	C		R		R			R			R	R	R	R	R	R														
60.23	C				R		R								R	R	R	R												
62.34	C		R	R			C				R		R																	
64.02	C														R				R	A	R									
65.74	C		R		R		R																							
66.21	A						R						R	R	R			R				R								
66.85	A		R	R	R		R	R											R											
67.05	C		R												C								C							
67.21	A		R		R						R				C							R								
67.40	A		R																											
67.59	A	R	R	R	C		R	R						R										R	C					
67.82	A		R					R	R	C	C			R	C	R	R							R		R	R	R	R	R
67.97	A								R							R														
68.42																											R			
69.12																														
73.21																														
UN-REMSA																														
SJS0001	A		C																											

Explanation: R: Rare (1–5), C: Common (6–19), A: Abundant (20+)

Table 3

Table 3.

Sample depth (m)	*Ambitisporites dilutus*	*Ambitisporites* spp.	*Dyadospora murusdensa*	Tetrad clusters	Tetrad indet.	Trilete spores	Verrucate spores	*Archaeozonotriletes* spp.	*Tetrahedraletes medinensis*	*Archaeozonotriletes chulus* var. *chulus*	*Lophozonotriletes* spp.	*Tetrahedraletes medinensis*	Reticulate spores	*Rugosphaera tuscarorensis*	*Tortotubus protuberans*
JA-2															
33.33															
46.20															
46.60	R	R	R	R	C	R	C								
48.18		R	C		A	R									
50.73		R	R		A	R	R	R							R
53.07		R	C		C	R			R						R
55.53	R		R		R	R		R	R						R
57.58	R		R		A		R		R	R	R	R	R	R	R
60.23		R			C										
62.34		R			A				R						R
64.02	R	R			C	R			R						R
65.74					C		R								C
66.21			R		C	R			R						
66.85					C				R					R	R
67.05			C		R				R						
67.21			C		C				R					R	
67.40			C		C			R	R						
67.59	C	R	R		A	C			R	R					R
67.82	C		R		A	C			R						R
67.97	R					A			R		R				R
68.42		R	C			C				R					R
69.12															
73.21															
UN-REMSA															
SJS0001	R				A										R

Explanation: R: Rare (1–5), C: Common (6–19), A: Abundant (20+)

Table 4

Table 4.

Sample depth (m)	Vitrinite –like, semistructered	Amorphous organic matter	Cutinite	Acritarchs	Inertinite	Vitrinite-like, degraded	Exinite spores	Exinite resinite	Exinite *Tasmanites*	Intertinite semifusinite
JA-2										
33.33	100									
46.20	100									
46.60	21	30	1	42	1	4				
48.18	20	35		40	1	1	3			
50.73	12	50		26	1		11			
53.07	15	50		31			4			
55.53	40	35		22				3		
57.58	30	44		18			8			
60.23	52	16		28			4			
62.34	34	38		24			3			
64.02	32	46		17			5			
65.74	25	61		11	1		2			
66.21	45	31		20			4			
66.85	5	63		25			7			
67.05	15	78		6			1			
67.21	55	18		27						
67.40	2	90		8						
67.59	50	6		19	6		19			
67.82	20	15		50		1	13		1	
67.97	22	45		27			6			
68.42	100									
69.12	80	11		8						1
73.21	100									
UN-REMSA										
SJS0001	5	89		2		2	2			

Table 5

Table 5.

Sample depth (m)	R_{ch} average	Corrected average	Count	Standard deviation	Minimum	Maximum	R_v calculated
46.60	0.59	0.57	49	0.029	0.54	0.65	0.44
46.60	0.56	0.55	66	0.036	0.48	0.63	0.41
48.18	0.60	0.58	4	0.021	0.58	0.62	0.45
57.58	0.55	0.56	72	0.043	0.47	0.63	0.41
64.02	0.63	0.63	20	0.031	0.58	0.68	0.48
64.02	0.63	0.61	22	0.065	0.55	0.74	0.48
65.74	0.50	0.49	74	0.031	0.45	0.55	0.36
65.74	0.54	0.53	22	0.019	0.52	0.57	0.40
67.82	0.52	0.51	5	0.026	0.49	0.55	0.38

Plate 1

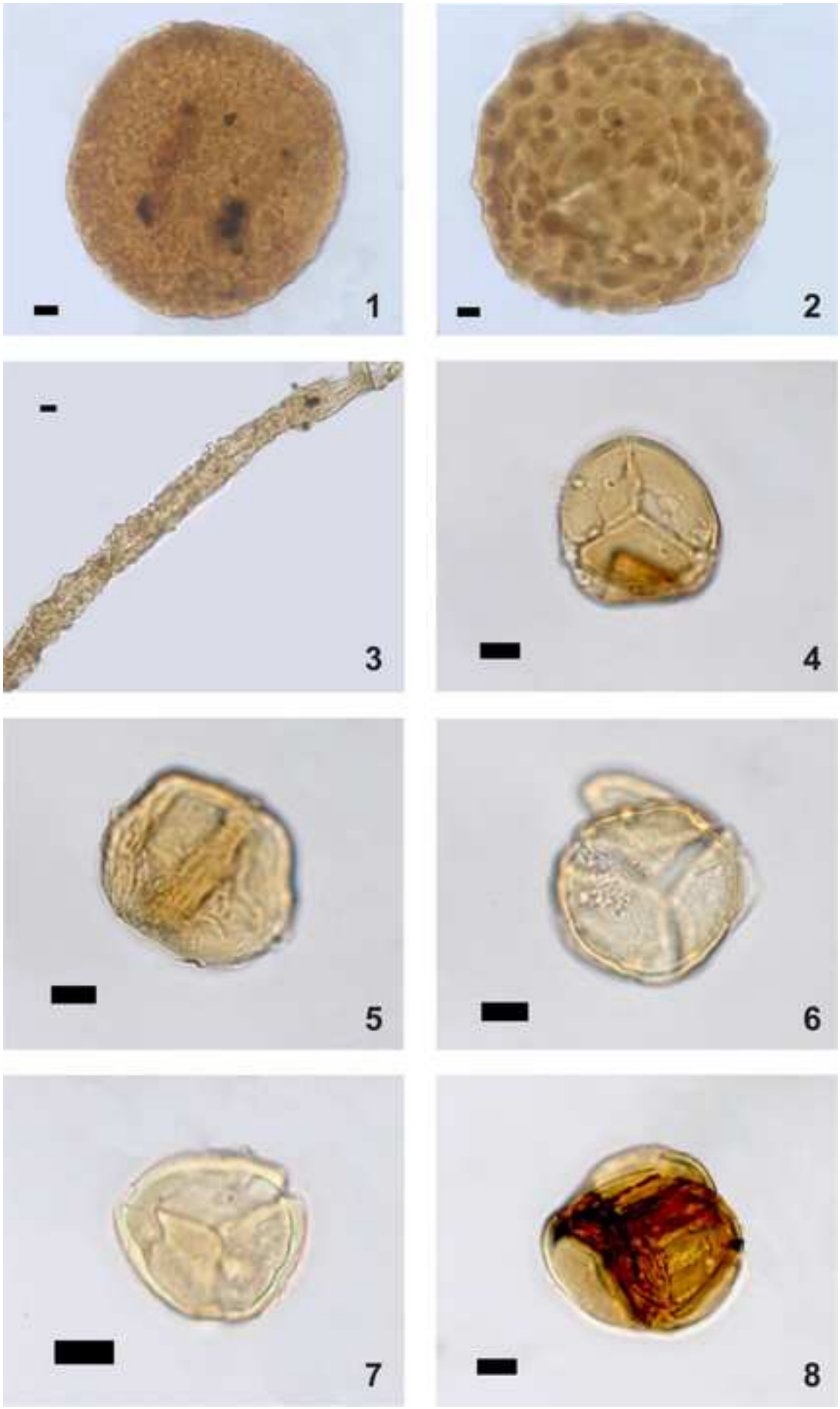

Plate 2

Plate 3

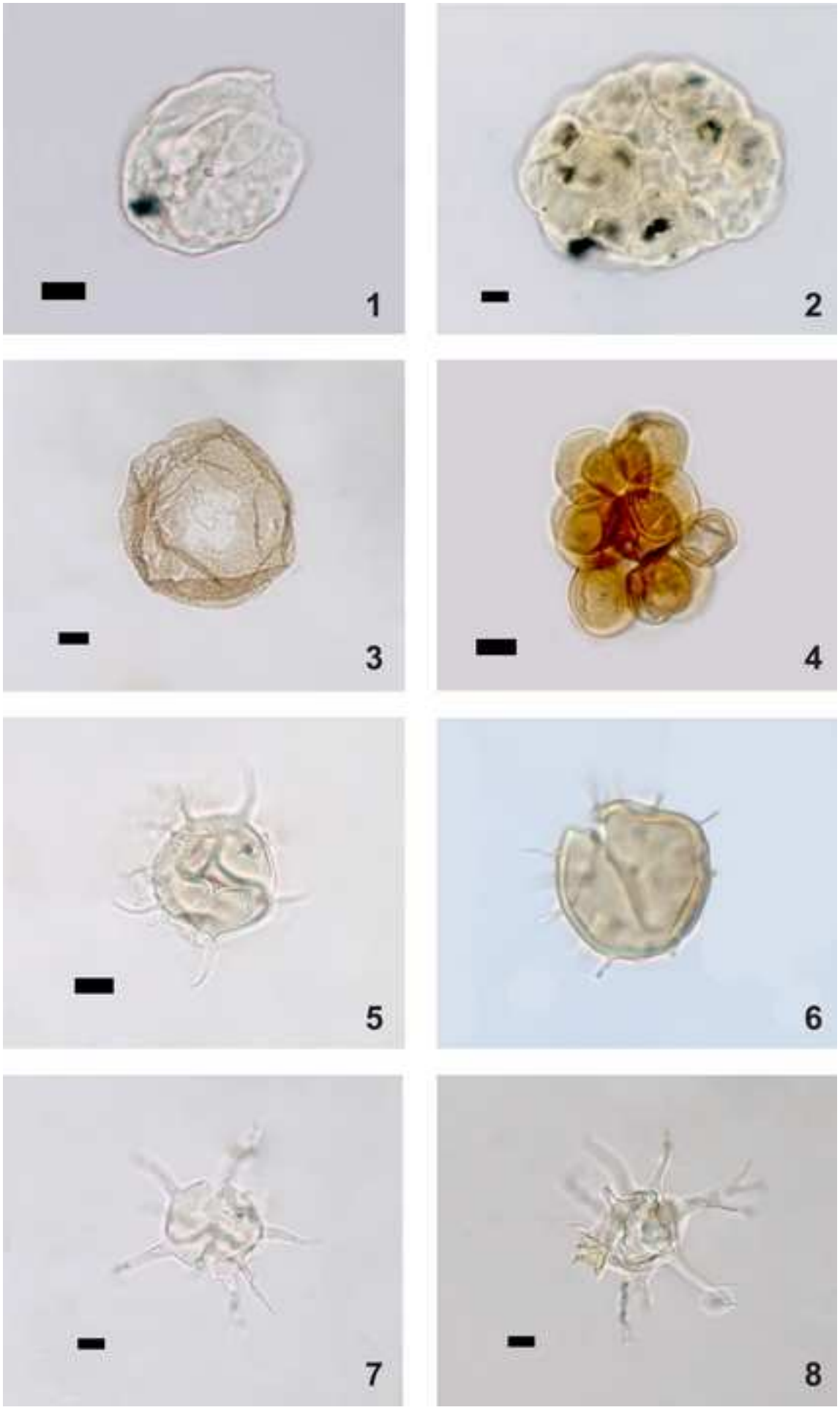

Plate 4

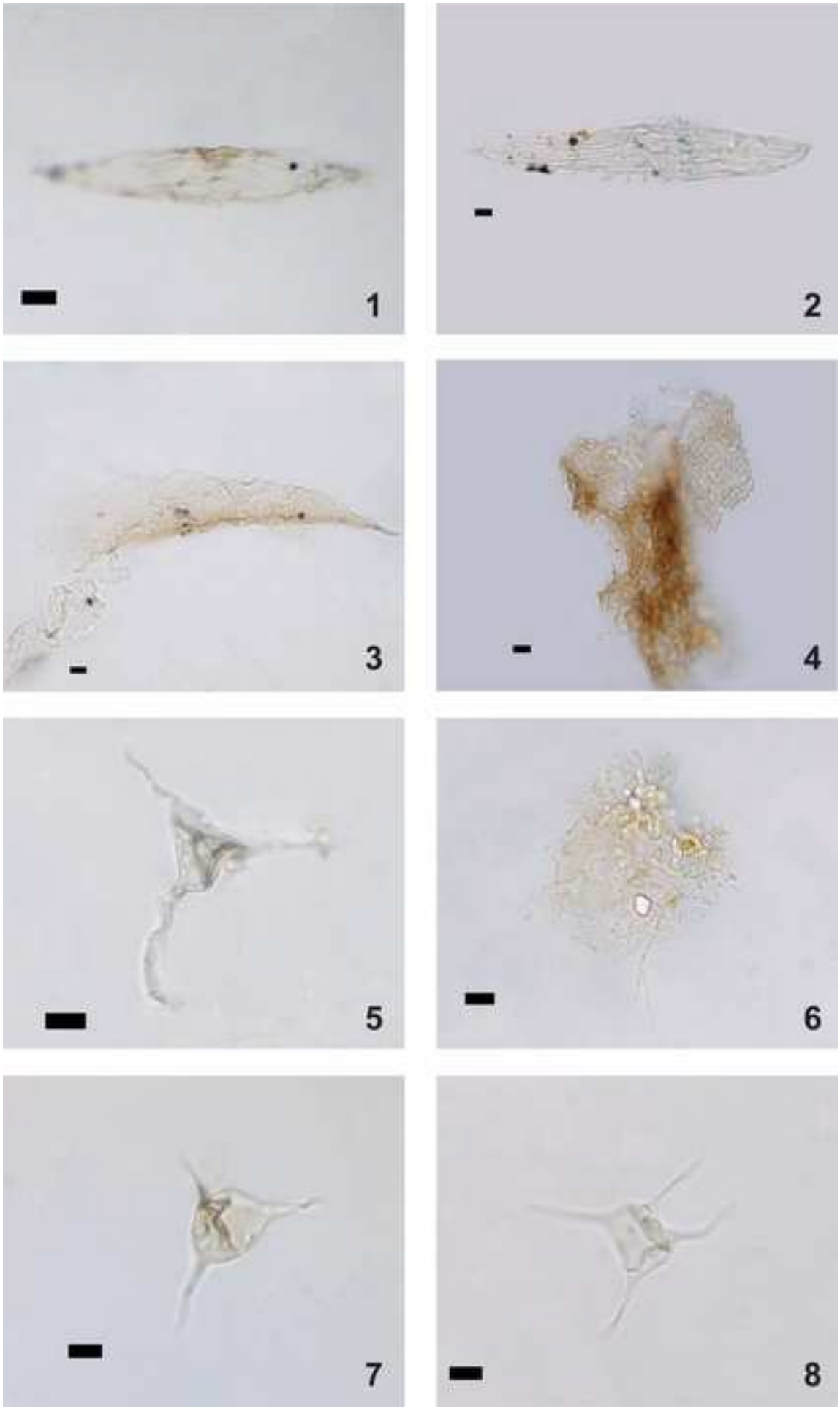

Plate 5

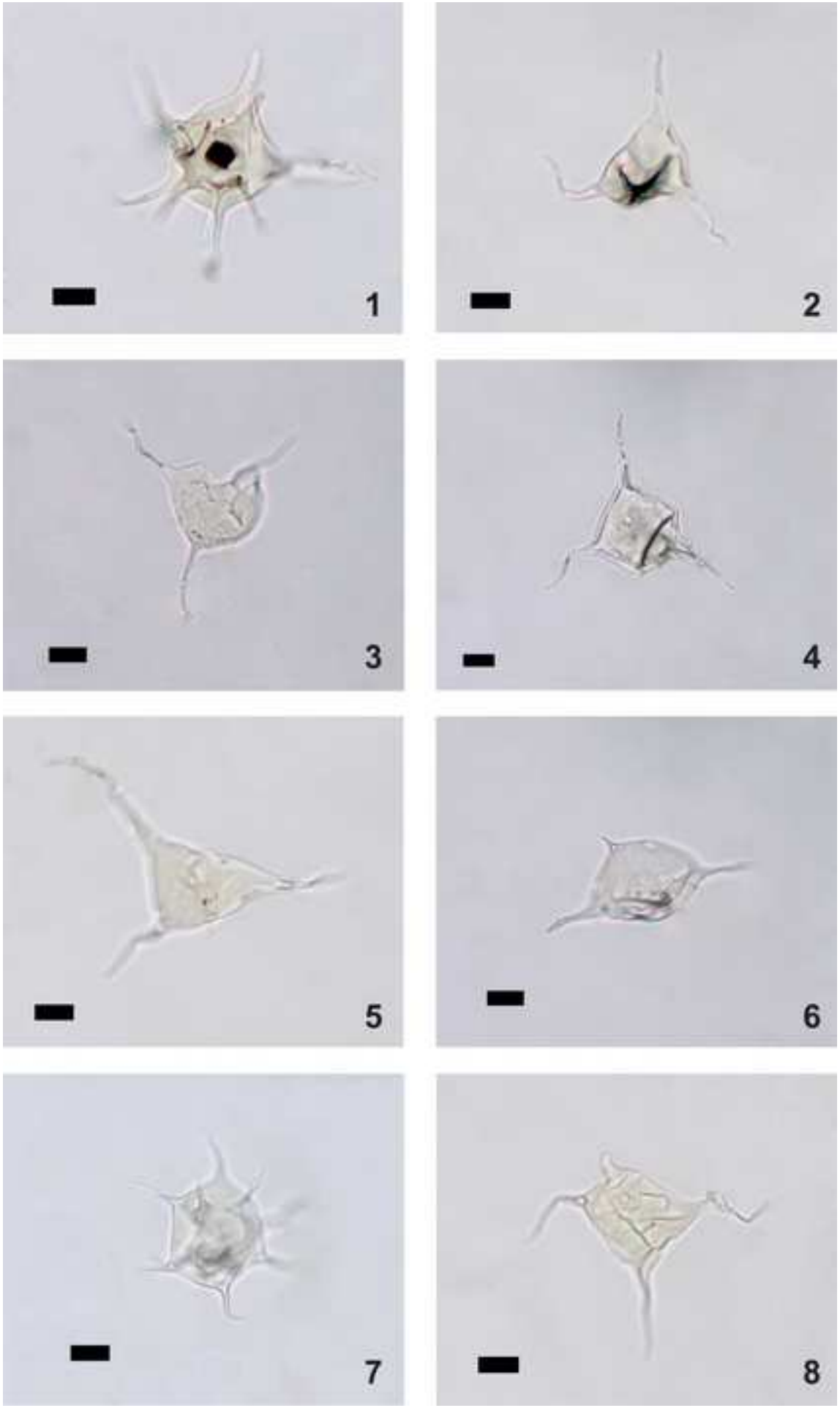

Plate 6

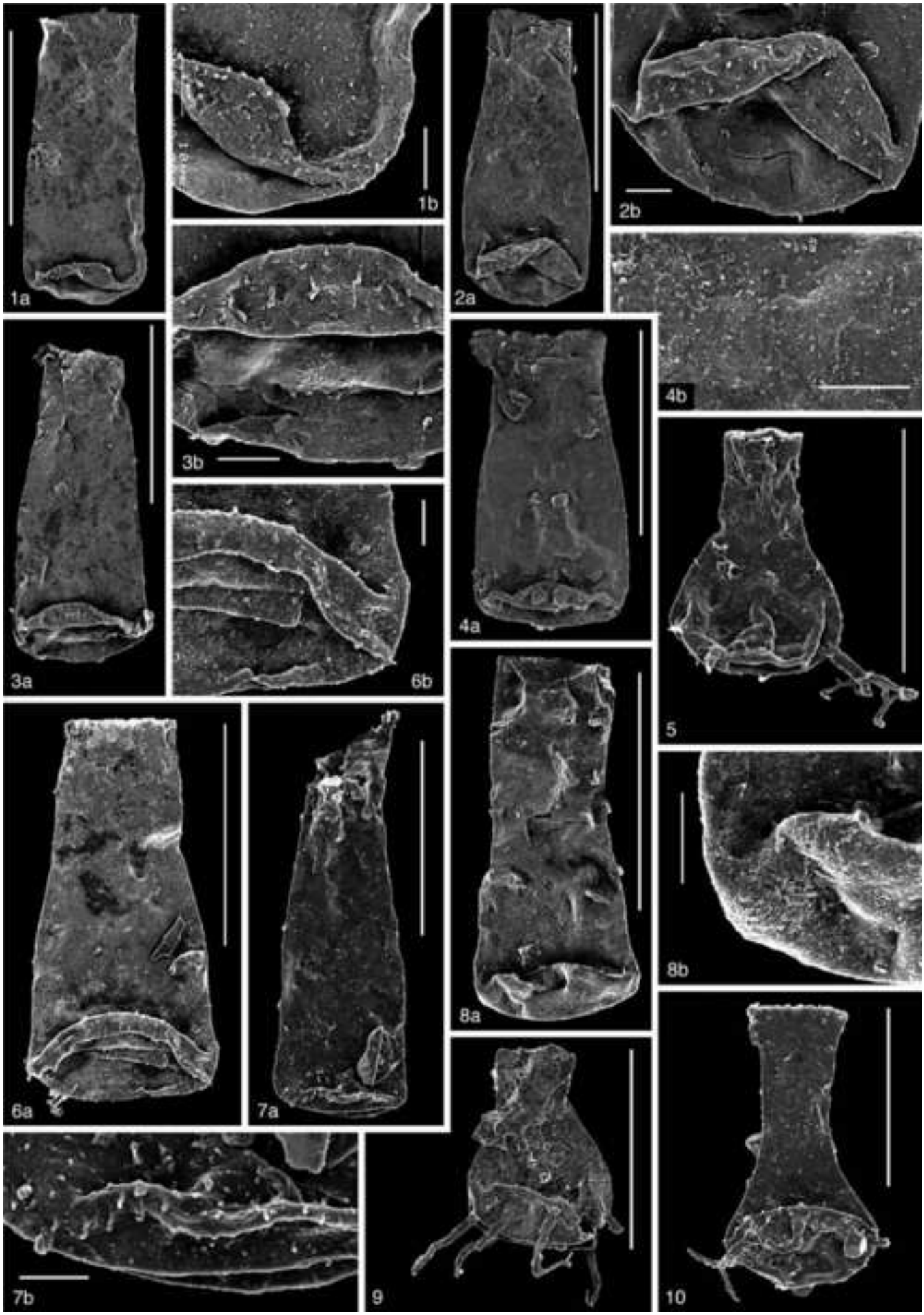

Plate 7

Click here to download high resolution image

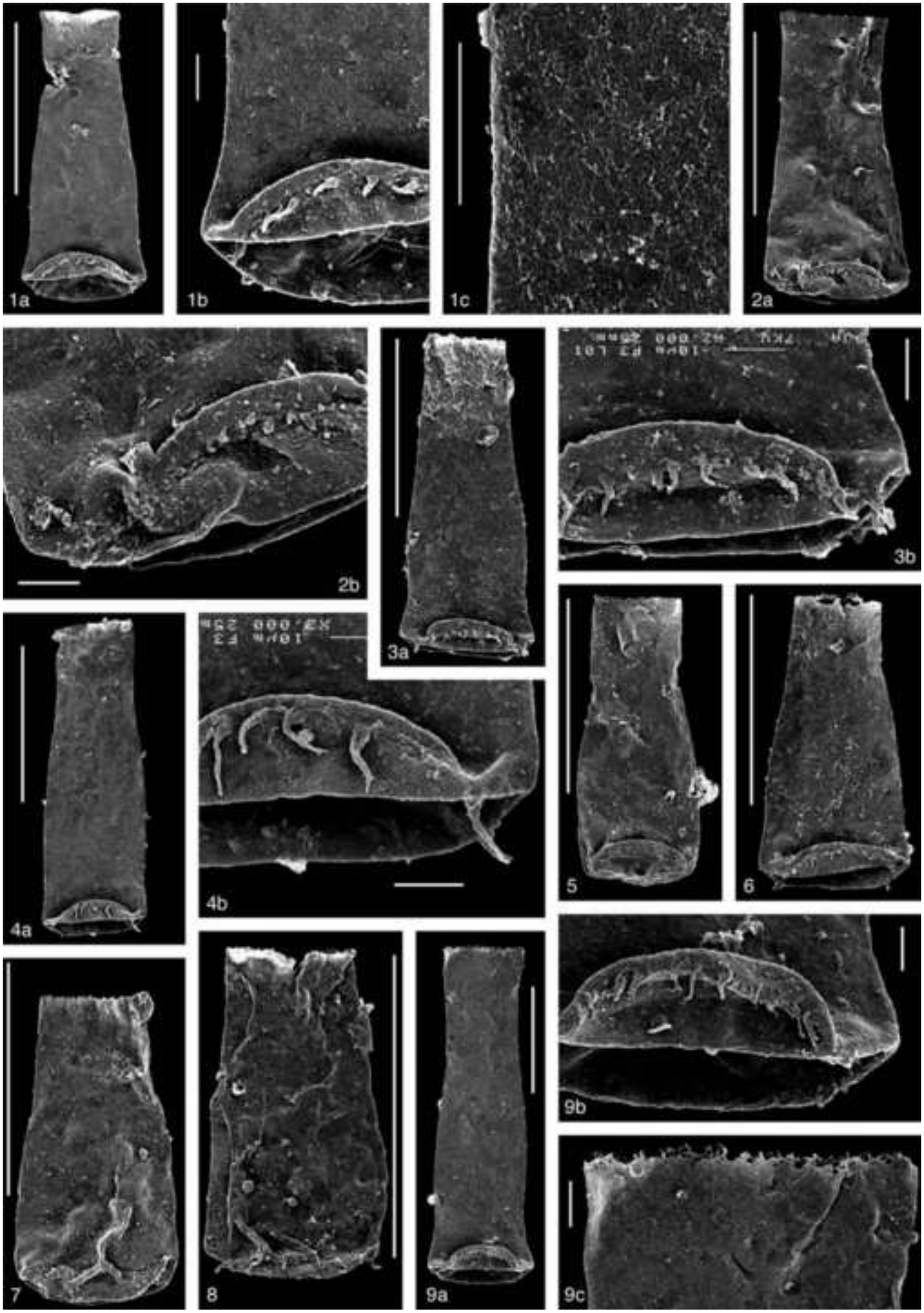

Plate 8

Click here to download high resolution image

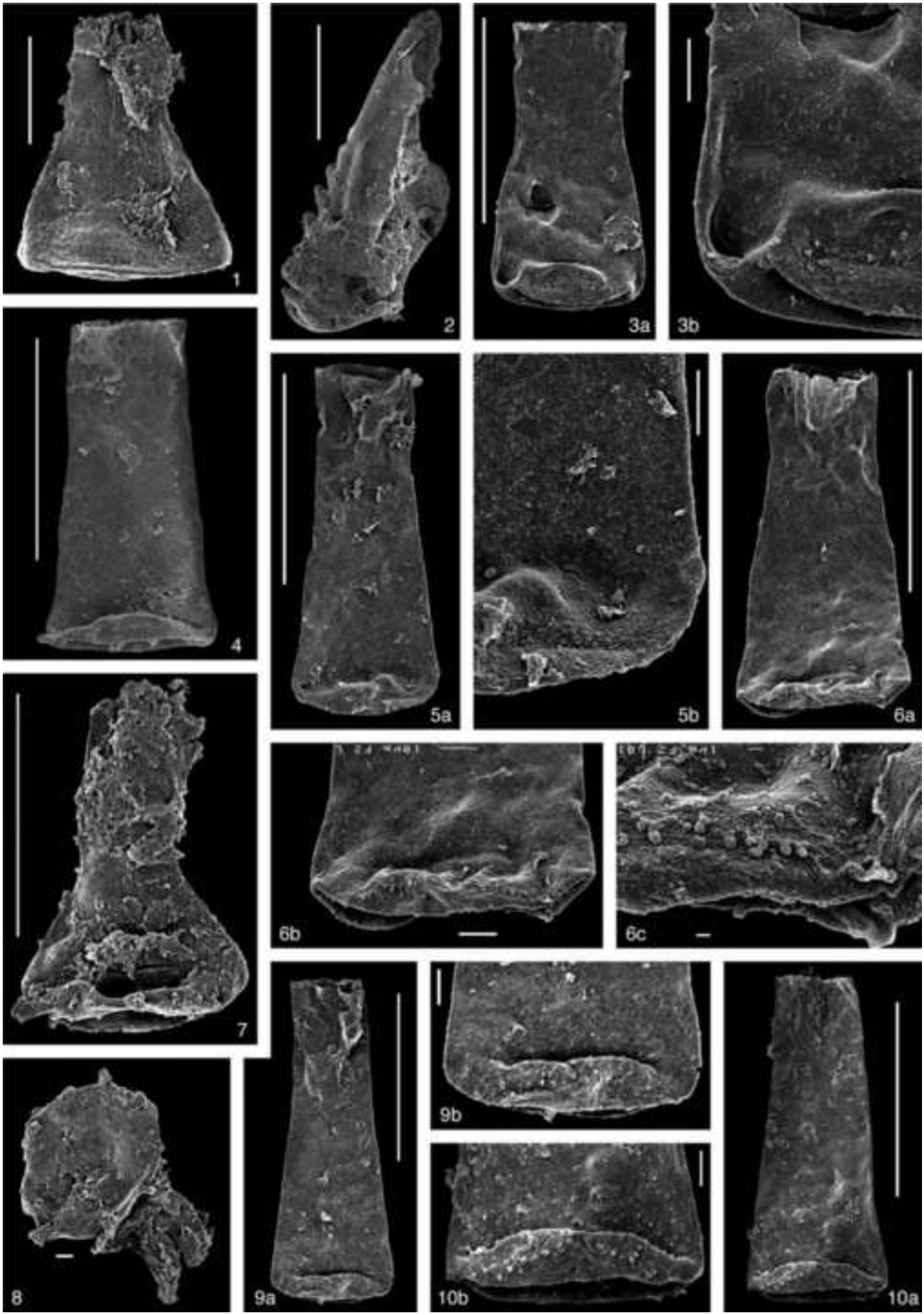

Plate 9

Click here to download high resolution image

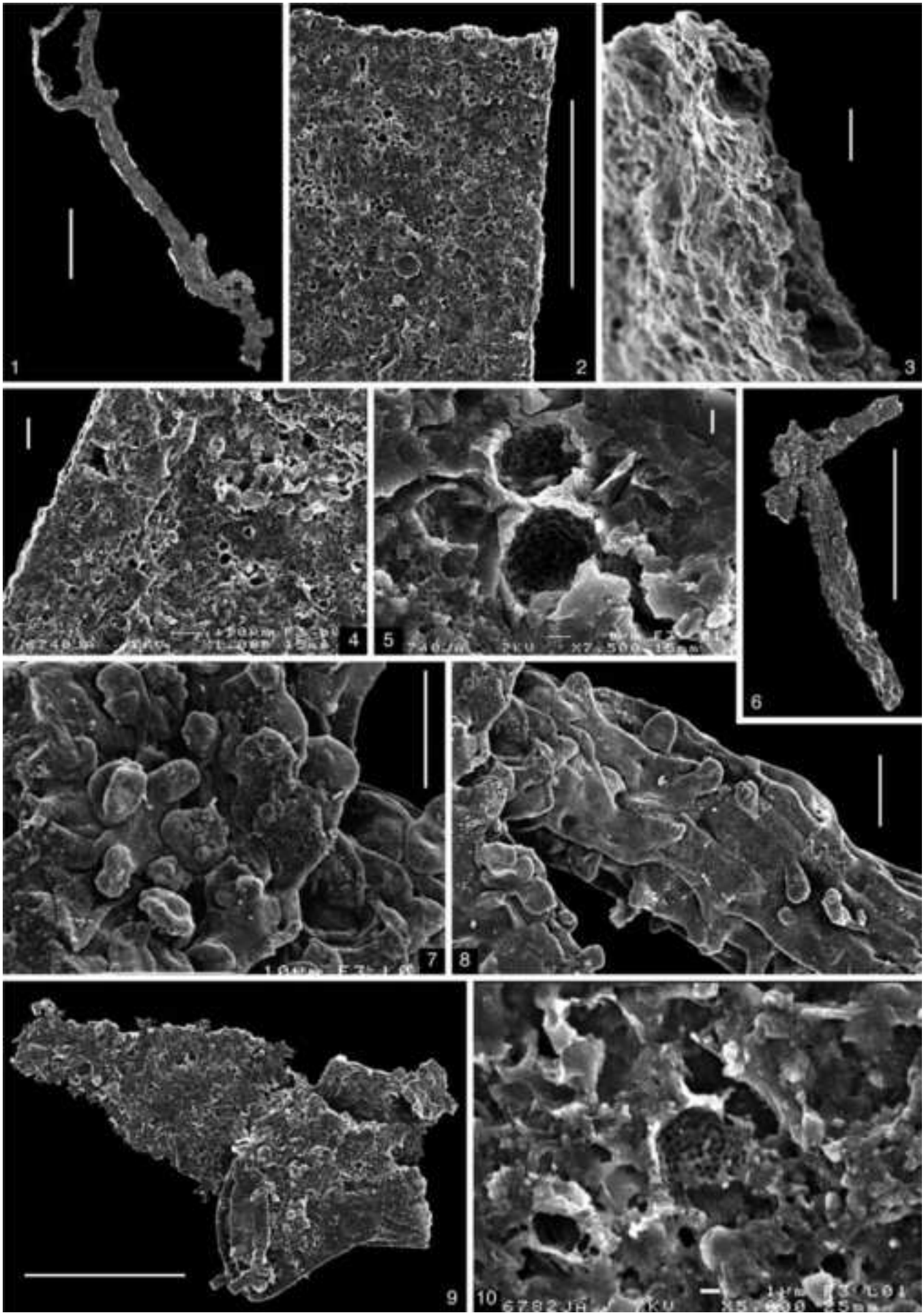

Plate 10

Click here to download high resolution image

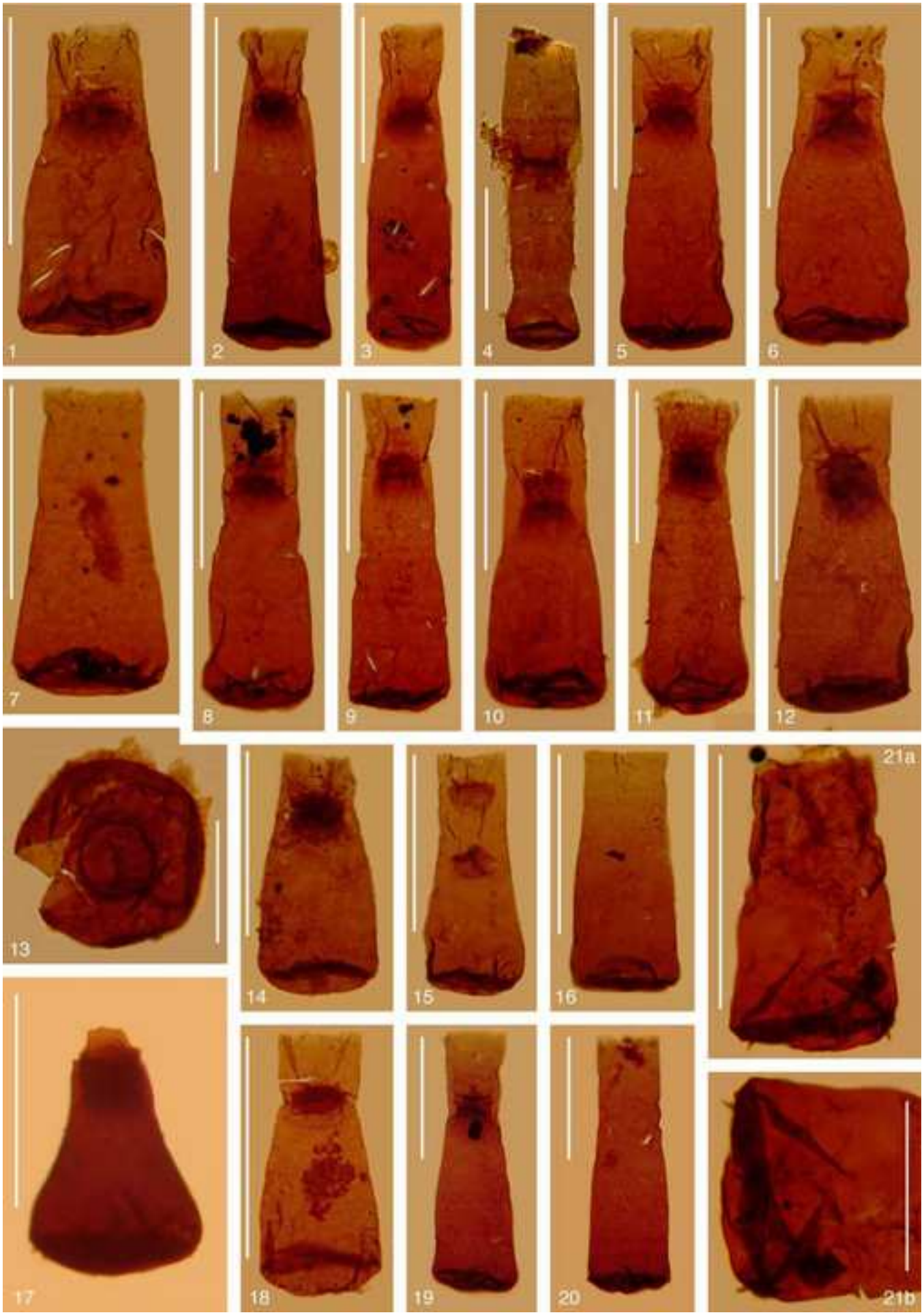

Plate 11

Click here to download high resolution image

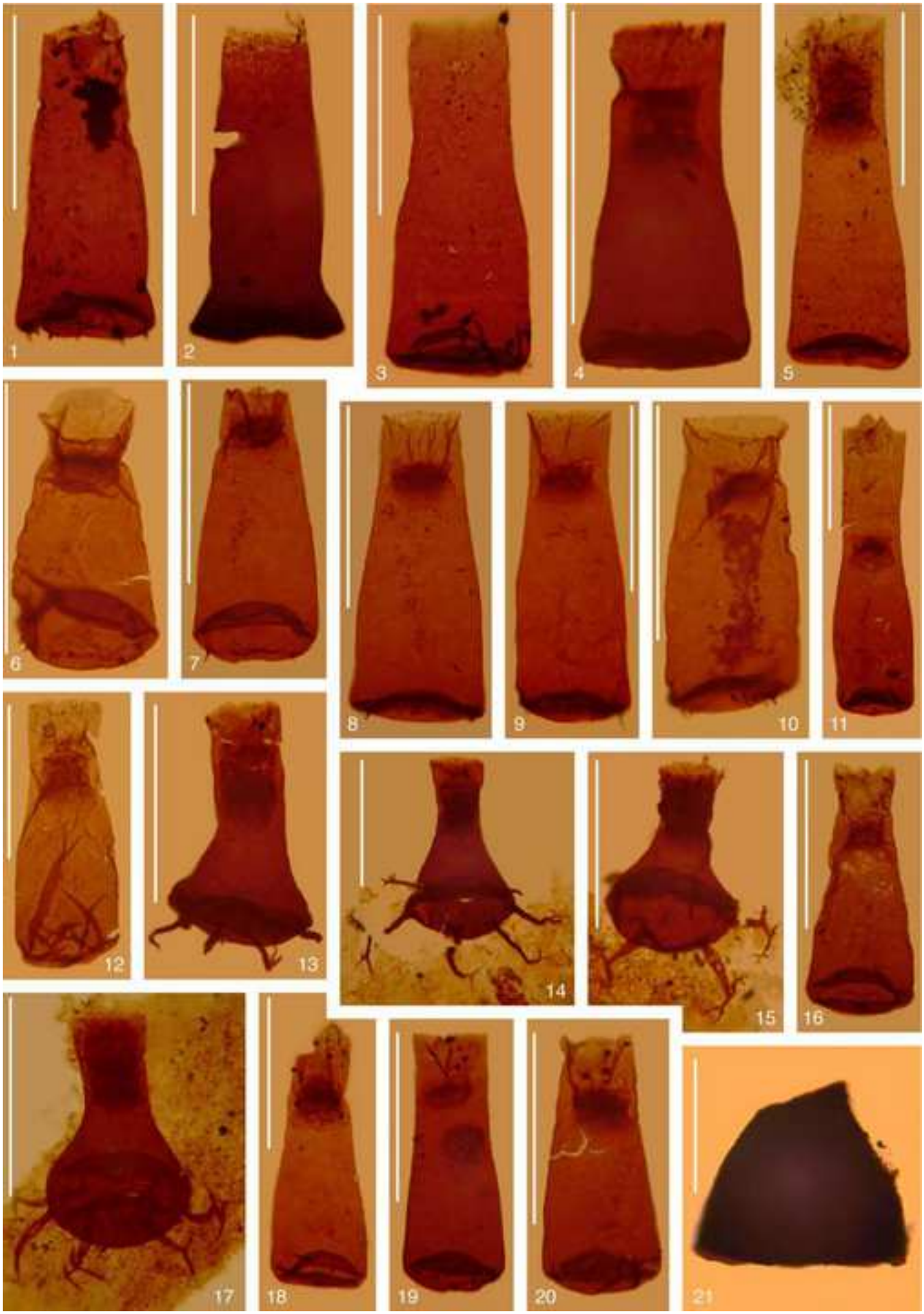

Plate 12

Click here to download high resolution image